

*Final Report*

## RESEARCH ON COLD CATHODES

*By:* D. V. GEPPERT    B. V. DORE

*Prepared for:*

NATIONAL AERONAUTICS AND SPACE ADMINISTRATION  
GODDARD SPACE FLIGHT CENTER  
GREENBELT, MARYLAND

CONTRACT NAS 5-9581

STANFORD RESEARCH INSTITUTE

MENLO PARK, CALIFORNIA



GPO PRICE \$ \_\_\_\_\_

CFSTI PRICE(S) \$ \_\_\_\_\_

Hard copy (HC) 3.00

Microfiche (MF) .50

FACILITY FORM 902

**N66 37363**

(ACCESSION NUMBER)

**57**

(PAGES)

**CR-78261**

(NASA CR OR TMX OR AD NUMBER)

(THRU)

(CODE)

**09**

(CATEGORY)

May 1966

*Final Report*

## RESEARCH ON COLD CATHODES

*Prepared for:*

NATIONAL AERONAUTICS AND SPACE ADMINISTRATION  
GODDARD SPACE FLIGHT CENTER  
GREENBELT, MARYLAND

CONTRACT NAS 5-9581

*By:* D. V. GEPPERT    B. V. DORE

*SRI Project 5511*

*Approved:* J. D. NOE, EXECUTIVE DIRECTOR  
ENGINEERING SCIENCES AND INDUSTRIAL DEVELOPMENT

*Copy No. ....5.*

NG6-37363

ABSTRACT

The requirements for the semiconductor, metal surface film and activator for the surface-barrier cathode are reviewed. The studies on GaP crystals and GaP/metal surface-barrier diodes conducted during the course of the program are reviewed and discussed. The activation experiments involving the evaporation of thin films of BaO on various metals are then reviewed and discussed. The recent experiments on nickel substrates indicate very-high-quantum-efficiency photoemission at elevated cathode temperatures.

The promising emission results obtained during the last quarter from transverse field emitters are presented. Alphas approaching 50 percent were obtained by subjecting thin films of evaporated BaO to high transverse fields ( $>10^5$  V/cm). These cathodes were operated under dc conditions, and emission current densities as high as about 1 amp/cm<sup>2</sup> were obtained.

*Author*

## CONTENTS

---

ABSTRACT. . . . .	ii
LIST OF ILLUSTRATIONS . . . . .	v
LIST OF TABLES. . . . .	vi
I INTRODUCTION . . . . .	1
II DISCUSSION . . . . .	4
A. Review of Requirements. . . . .	4
1. Semiconductor. . . . .	4
2. Surface Film . . . . .	5
3. Activation . . . . .	6
B. Semiconductor Studies . . . . .	7
1. GaP Characteristics. . . . .	7
2. GaP/Pt Diodes. . . . .	8
3. GaP/W Diodes . . . . .	10
4. GaP/Pd Diodes. . . . .	13
C. Activation Experiments. . . . .	17
1. Pt/BaO . . . . .	17
2. W/BaO. . . . .	19
3. Pd/BaO . . . . .	19
4. Ba/BaO . . . . .	19
5. Ni/BaO . . . . .	21
D. Alternate Cathode Structures. . . . .	22
1. Transistor Cathode . . . . .	22
2. The Transverse Field Cathode . . . . .	30
E. Emission Tests. . . . .	33
1. GaP/Pd/BaO Cathodes. . . . .	33
2. Si/BaO/Al Transverse Field Cathode . . . . .	33
F. Life Tests. . . . .	36
1. GaP/Pt Diode . . . . .	36
2. GaP/Pd Diode . . . . .	38
3. Ag/BaO Phototube . . . . .	39

III	CONCLUSIONS. . . . .	40
A.	Surface-Barrier Cathode . . . . .	40
B.	Transistor Cathode. . . . .	42
C.	Transverse Field Emitter. . . . .	43
D.	General Conclusions . . . . .	43
IV	RECOMMENDATIONS FOR FURTHER WORK . . . . .	45
A.	Schottky Barrier Cathode. . . . .	45
B.	Transistor Cathode. . . . .	45
C.	Transverse-Field Emitter. . . . .	45
	REFERENCES. . . . .	46

# ILLUSTRATIONS

Fig. 1	Energy Diagram of Surface-Barrier Cathode. . . . .	2
Fig. 2	Plot of Log I vs. V for GaP/Pt Diode . . . . .	9
Fig. 3	Plot of $1/C^2$ vs. V for GaP/Pt Diode. . . . .	10
Fig. 4	Square Root of Photoresponse per Photon vs. Photon Energy for GaP/Pt Diode . . . . .	11
Fig. 5	Plot of Log I vs. V for GaP/W Diode. . . . .	12
Fig. 6	Plot of $1/C^2$ vs. V for GaP/W Diode . . . . .	13
Fig. 7	Square Root of Photoresponse per Photon vs. Photon Energy for GaP/W Diode. . . . .	14
Fig. 8	Plot of Log I vs. V for GaP/Pd Diode . . . . .	15
Fig. 9	Plot of $1/C^2$ vs. V for GaP/Pd Diode. . . . .	16
Fig. 10	Square Root of Photoresponse per Photon vs. Photon Energy for GaP/Pd Diode . . . . .	16
Fig. 11	Square Root of Photoresponse per Photon vs. Photon Energy for Pt/BaO Phototube . . . . .	18
Fig. 12	Square Root of Photoresponse per Photon vs. Photon Energy for W/BaO Phototube. . . . .	20
Fig. 13	Square Root of Photoresponse per Photon vs. Photon Energy for Pd/BaO/Ba Surface (BaO deposited on heated substrate). . . . .	21
Fig. 14	Square Root of Photoresponse per Photon vs. Photon Energy for Ba/BaO Phototube . . . . .	22
Fig. 15	Photoresponse and Thermionic Emission as a Function of Temperature for Ni/BaO Cathode (BaO deposited on Ni at 600°C) . . . . .	23
Fig. 16	Photoelectric and Thermionic Emission Components as a Function of Anode Voltage for Ni/BaO Cathode (BaO deposited on Ni at 600°C). . . . .	24
Fig. 17	Spectral Response of Ni/BaO Cathode at Approximately 600°C (BaO deposited on Ni at 600°C) . . . . .	25
Fig. 18	Observed Photoresponse and Current Predicted from Fowler Analysis as a Function of Temperature for Ni/BaO Cathode . . . . .	26
Fig. 19	Energy Diagrams for Transistor Cathode . . . . .	27

Fig. 20	Response per Photon vs. Photon Energy for BaO-Activated GaAs . . . . .	28
Fig. 21	Variation in Response of BaO-Activated GaAs Crystal as a Function of Time. . . . .	29
Fig. 22	Schematic Drawing of M-I Transverse Field Emitter. . .	31
Fig. 23	Schematic Drawing of Alternative Transverse Field Semiconductor Emitter. . . . .	32
Fig. 24	Experimental Transverse-Field Cold-Cathode Structure .	34
Fig. 25(a)	Plot of Bias Current and Collector Current vs. Bias Voltage for Transverse-Field Emitter (Collector Voltage = 300V) . . . . .	35
Fig. 25(b)	Plot of Bias Current and Collector Current vs. Bias Voltage for Transverse-Field Emitter (Collector Voltage = 600V) . . . . .	36
Fig. 25(c)	Plot of Bias Current and Collector Current vs. Bias Voltage for Transverse-Field Emitter (Collector Voltage = 900V) . . . . .	37
Fig. 26	Plot of Collector Current vs. Collector Voltage For Transverse-Field Emitter (Bias Voltage = 89V, Bias Current = 30 $\mu$ A). . . . .	38
Fig. 27	Photograph of I-V Characteristics of GaP/Pd Diode on Life Test . . . . .	39
Fig. 28	Proposed Energy Diagram for a Thin Film of BaO on Metal . . . . .	41

# TABLE

---

Table 1	Evaluation of Barium-Oxide-Activation Experiments. . .	6
---------	--	---

## I INTRODUCTION

The objective of this program is to perform research on semiconductor/metal, hot-electron cold cathodes. The hot electrons are generated in a thin metal surface film by forward-biasing a rectifying semiconductor/metal diode. The metal film is on the order of 50-to-100 Å in thickness and is activated by a low-work-function coating to reduce the vacuum barrier below the semiconductor/metal barrier. Energy diagrams for the cathode, with and without bias, are shown in Figs. 1(a) and 1(b). (The structure is not drawn to scale and the thickness of the metal film is exaggerated for clarity.) Referring to Fig. 1(b), a portion of the hot electrons emitted over the top of the barrier into the metal film traverse the film ballistically and enter the vacuum. Most of the electrons that become scattered in the metal film are lost for our purposes, however, and these electrons create a bias current for the device.

Since the initiation of the contract, an alternative cold cathode has been suggested, as indicated in the Second Quarterly Report.<sup>1\*</sup> The energy diagrams for the new cathode, shown later, resemble those of an n-p-n transistor, and the operation of the cathode is similar to that of the transistor. The vacuum constitutes the collector for the transistor cathode, as it is called. The transistor cathode promises higher efficiency than the surface-barrier cathode.

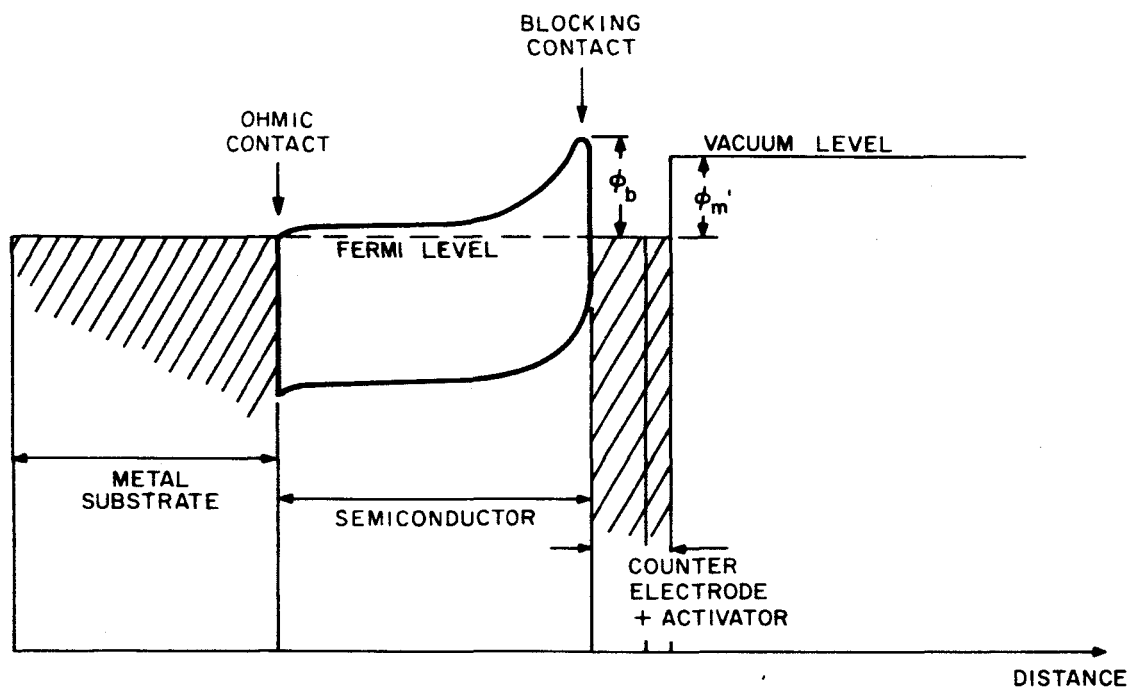
This report summarizes the work performance during the course of the contract, in addition to detailing the accomplishments of the last quarter.

Recently, a third cold-cathode concept has been investigated. This cathode is called a Transverse Field Emitter (TFE), and the results obtained from the initial tests indicate that high emission efficiencies

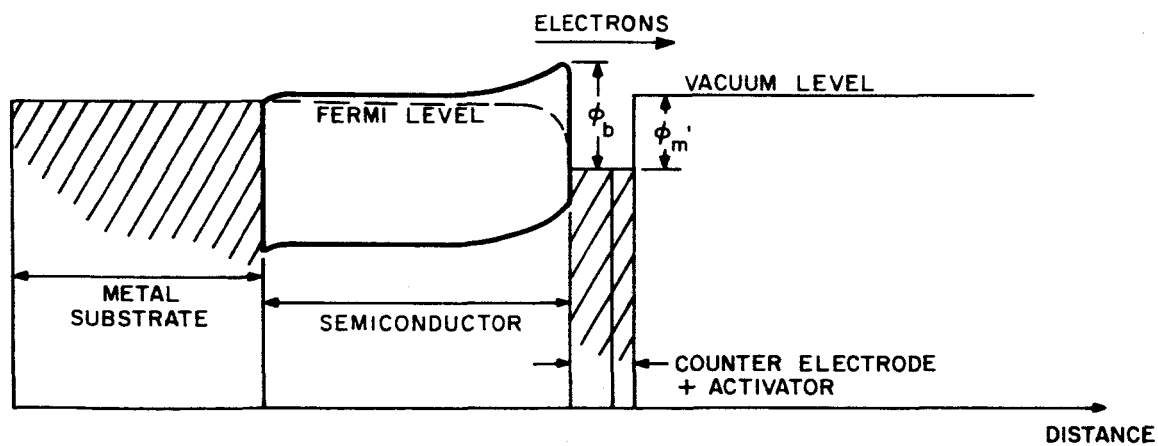
---

\*References are listed at the end of the report.





(a) ENERGY VS. DISTANCE OF SURFACE BARRIER CATHODE WITHOUT BIAS.



(b) ENERGY VS. DISTANCE OF SURFACE BARRIER CATHODE WITH BIAS.

TA-5511-50

FIG. 1 ENERGY DIAGRAM OF SURFACE-BARRIER CATHODE

are possible from such structures. The TFE will be described and discussed in detail in Sec. II-D-2.

## II DISCUSSION

### A. Review of Requirements

The operation of the surface-barrier cathode is illustrated in the energy diagram of the structure with bias applied [Fig. 1(b)]. Electrons are injected into the conduction band of the barrier layer at the ohmic contact these electrons diffuse through the semiconductor toward the blocking contact. In the high-field region in the vicinity of the metal/semiconductor barrier they acquire the energy necessary for emission into vacuum. This assumes that the metal/vacuum barrier  $\phi'_m$  is less than the metal/semiconductor barrier  $\phi_b$ , and that the electrons traverse the thin metal film with no loss in energy. More detailed requirements for the semiconductor, the metal surface film and the vacuum barrier will be considered in the following sections.

#### 1. Semiconductor

The primary requirement for the semiconductor is the formation of high surface barriers with various metals. In addition, the semiconductor has to have a relatively large bandgap ( $\sim 2.0$  eV) to minimize hole injection from the metal surface film. The semiconductor must be capable of being doped n-type to a reasonably low resistivity. Finally, it must be possible to make ohmic contacts to this material, which should be available in single crystals large enough for useful cathodes.

One of the difficulties in selecting suitable semiconductors for this application was the lack of a semiconductor/metal model that was consistent with experimental results. Accordingly, an analysis was made of the correlation between barrier heights and metal work functions, which included the effects of surface states (Appendices B and C, First Quarterly Report<sup>2</sup>). This analysis is being published in revised form in the May 1966 issue of the Journal of Applied Physics.<sup>3</sup> In summary, the Schottky relation for barrier height,

$$\phi_b = \phi_m - E_A \quad (1)$$

where  $E_A$  is the electron affinity of the semiconductor, is modified by the addition of a  $V_3$  term to account for surface states. When image-force lowering of the barrier is included, the approximate expression for barrier height becomes:

$$\phi_b \approx (\phi_m - E_A - \Delta \phi_n) + V_3 \quad . \quad (2)$$

It is important to use  $\phi_m$  values for thin films of the metal in question as measured on single crystals of the semiconductor under consideration. For high-work-function metals like Pd, Pt, and Au on GaAs, the barrier height is "pinned" at 0.85 to 0.90 eV because of surface states at the Fermi level.

Two semiconductor materials for the surface-barrier cathode were considered in a previous study.<sup>4</sup> These were single crystal and polycrystalline ZnO and thermally grown  $\text{TiO}_2$ . In the current program a brief evaluation of some  $\alpha$ -SiC was made, but the major effort was concerned with single crystal GaP. The experimental results with the latter material will be reviewed in Sec. II-B.

## 2. Surface Film

The need for a high semiconductor/metal barrier was explained above. This requirement favors metals with higher work functions, but there are other considerations. The need for a low metal/vacuum barrier appears to contradict the first requirement. However, the results obtained in activating various metal films with BaO indicate that the initial work function of the metal is of little consequence (Table I).

The surface film has to be thin enough to allow the hot electrons to traverse it with a minimum loss in energy. Considering the values of hot-electron mean free path that have been measured for some metals, the surface film should be less than 100 Å in thickness for efficient operation. Since the lateral conductivity is poor for such films, a gridded surface design was adopted in this study. Relatively thick metal stripes connected by an annular deposit were evaporated first. This was followed by a thin overlay of the same metal just before the activation cycle.

Table I

## EVALUATION OF BARIUM-OXIDE-ACTIVATION EXPERIMENTS

Substrate Film	$\phi_1^*$ (initial)	Average $\phi_2$ (final)	$\phi_2/\phi_1$	$\phi_1 - \phi_2$
Ag	4.31 eV	1.48 eV	0.29	2.83 eV
Pt	5.48 eV	1.66 eV	0.30	3.82 eV
W	4.36 eV	1.44 eV	0.33	2.92 eV
Pd	4.95 eV	1.46 eV	0.295	3.49 eV
Ba	2.50 eV	1.48 eV	0.59	1.02 eV
Mo	4.22 eV	1.75 eV	0.415	2.47 eV

\* Average of recent measurements on thin films of the metal.

The effect of traces of pump oil on the semiconductor/metal barrier was discussed in the Second Quarterly Report.<sup>1</sup> Most of the GaP/metal diodes were made in oil-free systems; the diode characteristics obtained with various metals will be considered in Sec. II-B. The metals used were Pt, W, and Pd, which have high melting points. Thin films of these metals can withstand bake-out cycles without agglomerating, which is another consideration in selecting materials for this structure.

### 3. Activation

Since the metal/semiconductor barriers attainable with GaP are in the vicinity of 1.5 eV, the metal surface film has to be activated to produce a metal/vacuum barrier less than this value. The material used for this purpose should be relatively easy to apply to facilitate reproducibility. It should also be capable of withstanding the processing schedules that are used in fabricating the tubes that utilize this cathode. The activated surface should be stable in the type of vacuums that are attainable with current technology.

Evaporated films of BaO appear to meet most of these requirements. This material has been used in this laboratory for the past two years on this and related programs. Various techniques for optimizing the activation process have been developed. These techniques and the experimental results obtained on various metals will be reviewed in Sec. II-C.

## B. Semiconductor Studies

### 1. GaP Characteristics

Most of the n-type GaP used in this investigation was obtained from Monsanto Chemical Company. One sample from Stanford University was used in the earlier work on the program. The properties and preparation of the crystals will be summarized in this report. Detailed information will be found in the quarterly reports, particularly in the First Quarterly Report.<sup>2</sup>

The Stanford University crystal was doped with sulfur and had a resistivity of 0.38 ohm-cm. The Monsanto crystals were doped with tellerium and a number of diodes were made from a crystal having a resistivity of 0.079 ohm-cm. Hall measurements were made on both crystals and values of 110 and 125 cm<sup>2</sup>/volt-s were obtained. Optical transmission measurements produced bandgap energies in the range of 2.15 to 2.22 eV.

It was found that the "A" (gallium) side of the crystal will etch to a mirror finish in hot aqua regia, but will pit and scratch very easily by mechanical abrasion. The "B" (phosphorus) side takes a good mechanical polish and etches to a matt finish in hot aqua regia. A flat, uniform mirror finish prior to etching was obtained with a Buehler AB Texmet polishing cloth backed by a glass plate. A slurry of alumina in deionized water is used, starting with 5-micron particle size followed by 0.3-micron particles.

A paragraph from the First Quarterly Report<sup>2</sup> regarding the toxicity of GaP in polishing operations is included here as a precaution for anyone contemplating the use of this material.

"Lapping and polishing operations on gallium phosphide are accompanied by the release of phosphine gas. This is associated with any mechanical abrading process, which apparently enhances the formation of poisonous phosphorus compounds through catalytic action. Phosphine gas is very high in toxicity, and the maximum allowable concentration is 0.05 ppm. Concentrations well below the maximum are easily detected as phosphine has a strong characteristic odor which becomes noticeable at very low concentration levels. Because of the toxic qualities of the lapping and polishing products, all mechanical operations should be done in a fume hood with a flow rate sufficient to maintain concentrations below the maximum allowable values."

Ohmic contacts to the GaP have been formed by alloying metallic lead or tellurium-doped silver to the "B" side of the crystal. Lead is convenient for laboratory tests, but the lower-vapor-pressure material is required for high-vacuum operation. A small piece of silver doped with 1 percent tellurium is preformed by heating into a ball approximately 10 mils in diameter. This is alloyed into the GaP at about 900°C in a dry hydrogen atmosphere.

## 2. GaP/Pt Diodes

Detailed results on GaP/Pt diodes were included in the First Quarterly Report.<sup>2</sup> The significant feature that came out of the analysis of these results was evidence of a contaminating film between the Pt and the GaP. A semilog plot of current vs. voltage for one of these diodes (Fig. 2) produced a value of  $n$  of about 3.5. In the straight-line portion of this plot where  $I \propto \exp [qV/nkt]$ ,  $n$  should be unity according to simple Schottky theory. When the straight-line reverse-bias portion of a plot of  $1/C^2$  vs.  $V$  was extrapolated (Fig. 3), an intercept much larger than the barrier height was obtained. The donor density in the GaP calculated from the slope of this plot was in good agreement with a previous value calculated from resistivity and mobility measurements. The intercept from a plot of the square root of the response per photon vs. photon energy (Fig. 4) agreed with the intercept from the forward-bias portion of the plot of  $1/C^2$  vs.  $V$  shown in Fig. 3.

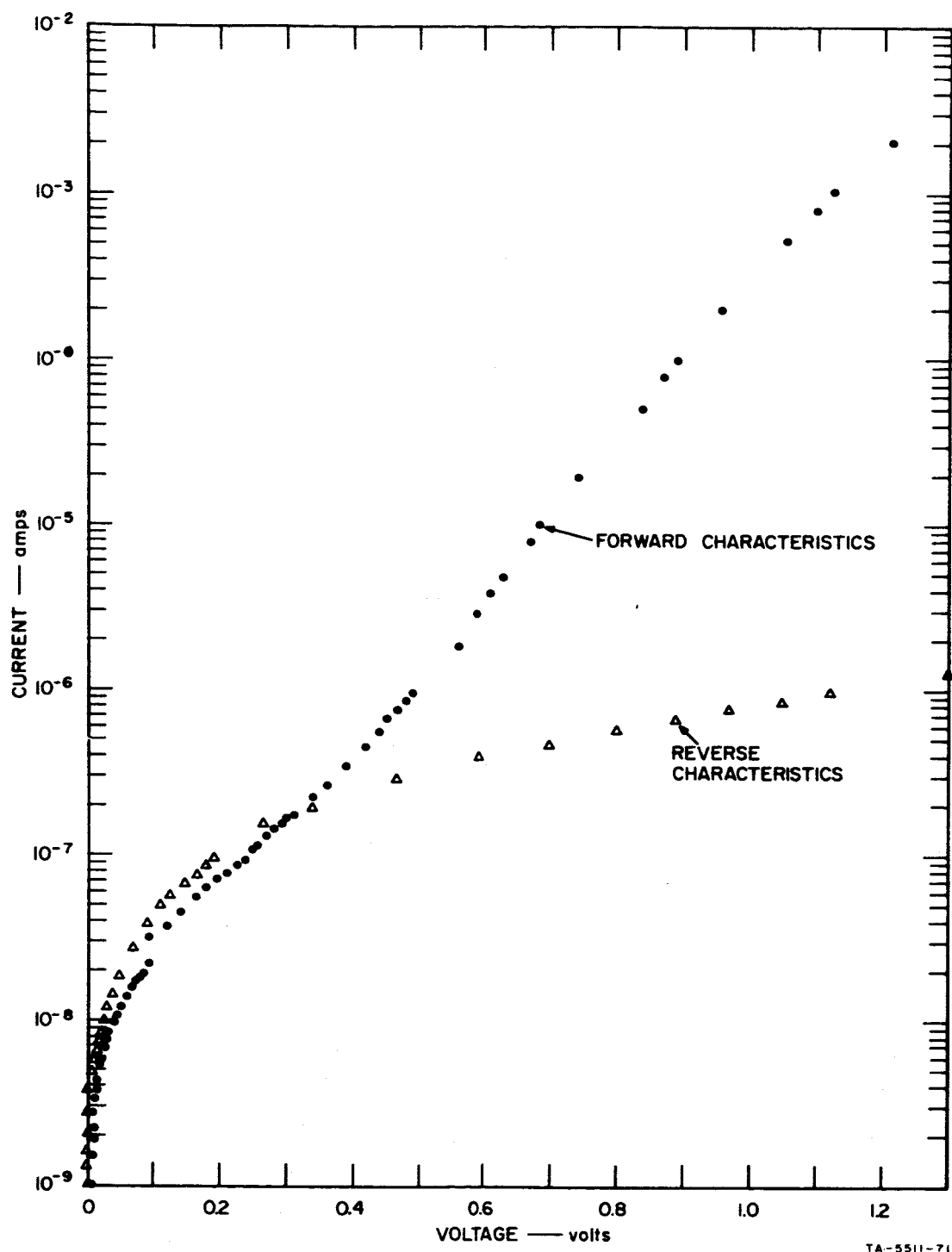


FIG. 2 PLOT OF LOG I vs. V FOR GaP/Pt DIODE



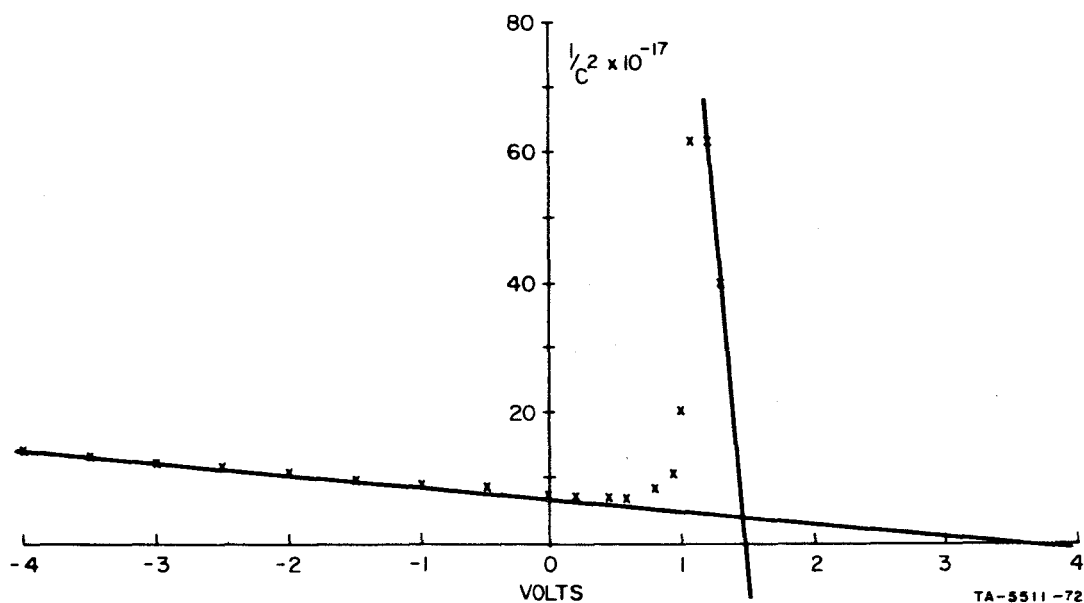
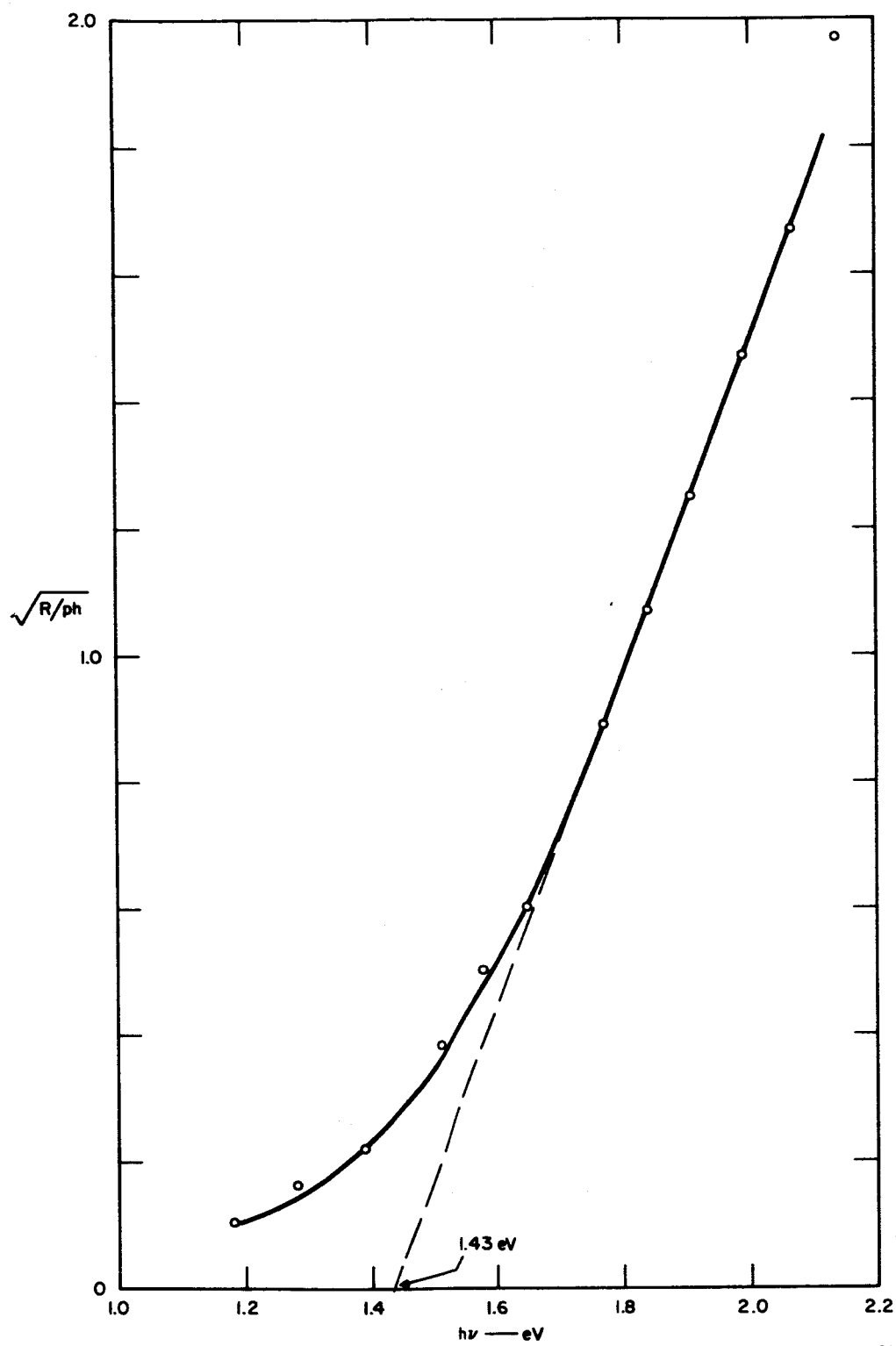


FIG. 3 PLOT OF  $1/C^2$  vs. V FOR GaP/Pt DIODE

Since the Pt was evaporated in an oil-pumped vacuum system at a pressure of about  $10^{-6}$  torr, it was concluded that the contamination was due to oil. All subsequent GaP diodes were fabricated in oil-free systems.

### 3. GaP/W Diodes

When it was found that the lowest Pt/BaO vacuum barriers attainable were not compatible with the GaP/Pt barriers, it was decided to try W in place of the Pt. The results obtained with GaP/W diodes were included in the Second Quarterly Report.<sup>1</sup> Some difficulty was experienced in evaporating W, but the diodes that were tested had the best characteristics of all the GaP/metal diodes made in this program. the value of  $n$  from the semilog plot of current vs. voltage in Fig. 5 is about 1.7. Although the diode does not follow simple Schottky theory, this value of  $n$  is lower than that obtained with the GaP/Pt diodes. This may be due in part to eliminating the oil contamination by using an ion-pumped system for the W experiments.



TB-5511-73

FIG. 4 SQUARE ROOT OF PHOTORESPONSE PER PHOTON vs. PHOTON ENERGY FOR GaP/Pt DIODE

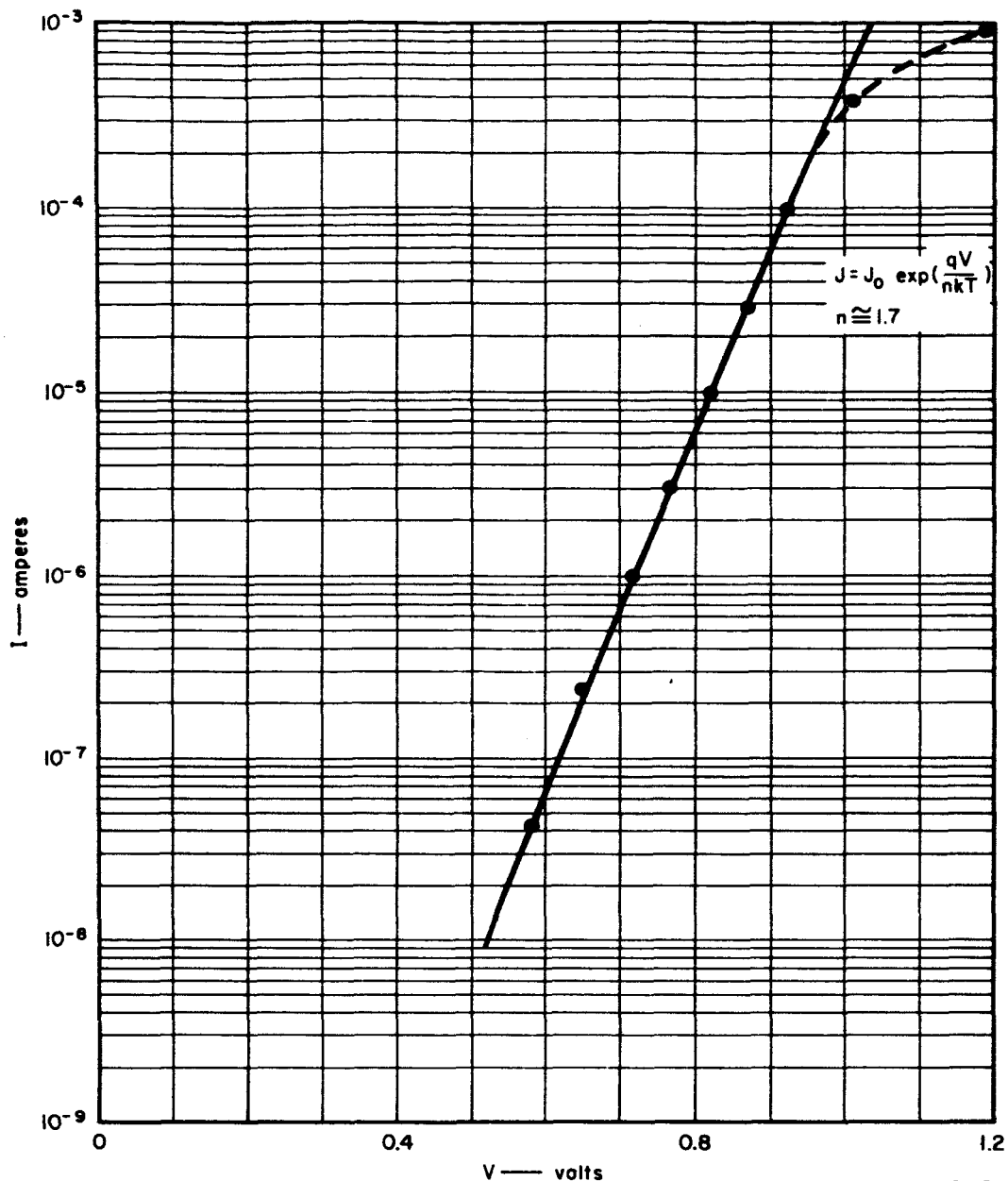


FIG. 5 PLOT OF LOG I vs. V FOR GaP/W DIODE

The  $1/C^2$  vs. V plots and the spectral-response data confirm the nonuniform barrier model for these diodes. The intercept from the plot of the  $1/C^2$  vs. V is 1.5 eV (Fig. 6), but the capacitance appears to go infinite at about 0.8 eV. The square root of the response per photon vs. photon energy has a long low-energy tail which makes it

difficult to obtain a well-defined intercept. A range of values between 1.3 eV and 1.5 eV can be selected from the plot in Fig. 7.

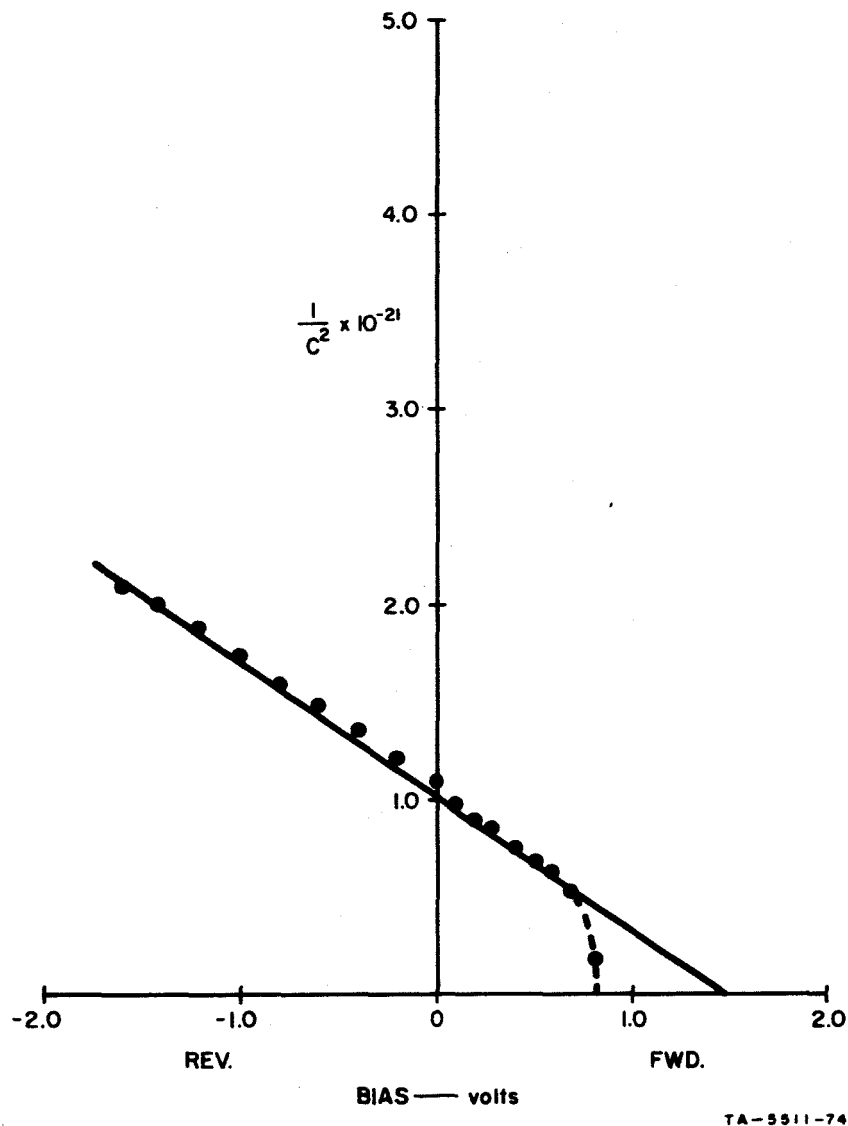


FIG. 6 PLOT OF  $1/C^2$  vs.  $V$  FOR GaP/W DIODE

#### 4. GaP/Pd Diodes

Although good GaP/W diodes were made and tested, the difficulties in evaporating W led to the selection of another metal. Based upon the theory developed by Geppert, Cowley, and Dore,<sup>3</sup> Pd appeared to be a

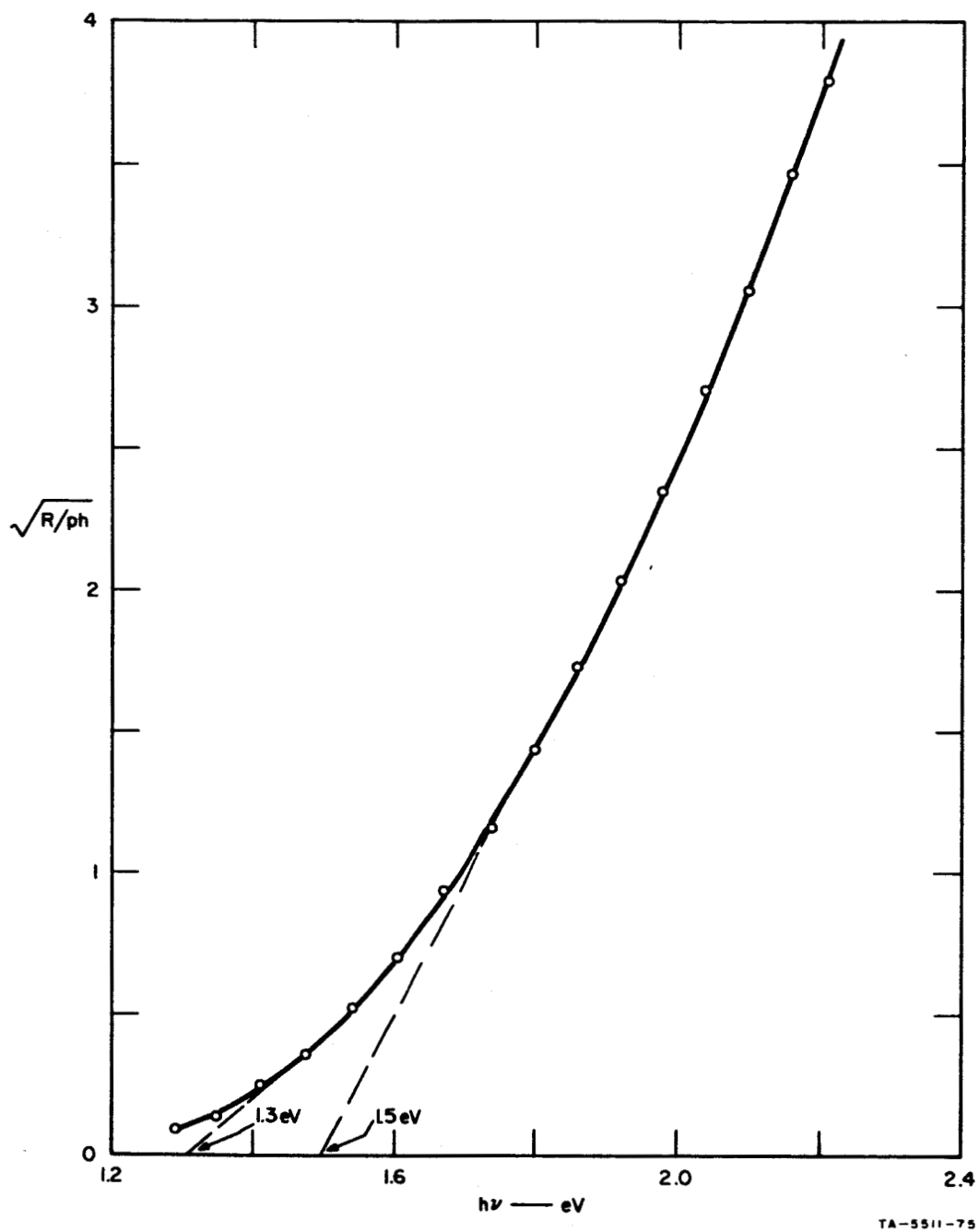


FIG.7 SQUARE ROOT OF PHOTORESPONSE PER PHOTON vs. PHOTON ENERGY FOR GaP/W DIODE

reasonable choice. A number of diodes were fabricated and the results of measurements made were reported in the Third Quarterly Report.<sup>5</sup> One diode was placed on life test and its performance is described in Sec. II-F-2.

A typical I-V characteristic is shown in Fig. 8, and again there are indications of nonuniform barriers resulting in high currents

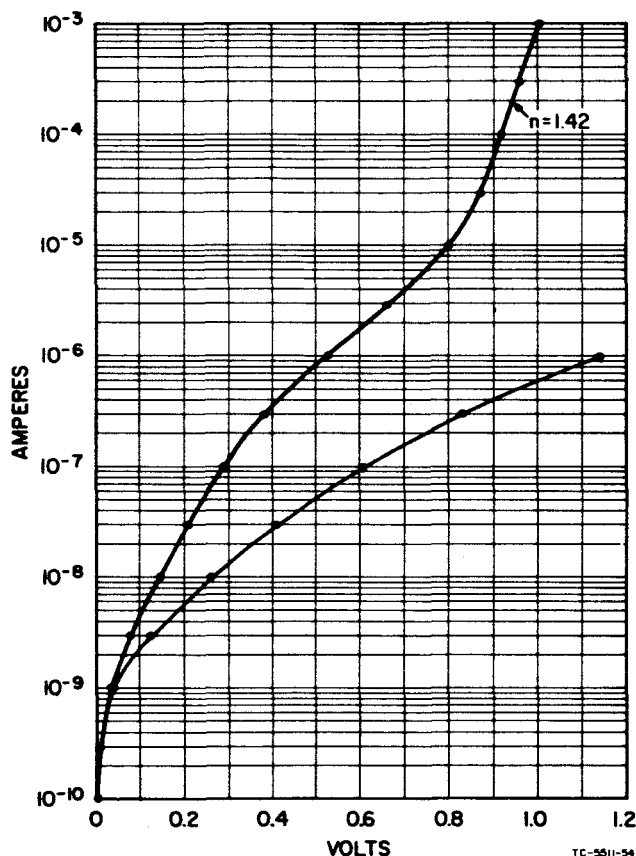


FIG. 8 PLOT OF LOG I vs. V FOR GaP/Pd DIODE

at low bias voltages. The plot of  $1/C^2$  vs. V in Fig. 9 goes to zero at one volt forward bias and the intercept indicates a diffusion potential of approximately 1.3 eV. A range of values between 1.40 and 1.55 eV was obtained from spectral-response measurements. Figure 10 has a unique intercept at 1.475 eV, but the long low-energy tail indicates regions in the barrier having lower values.

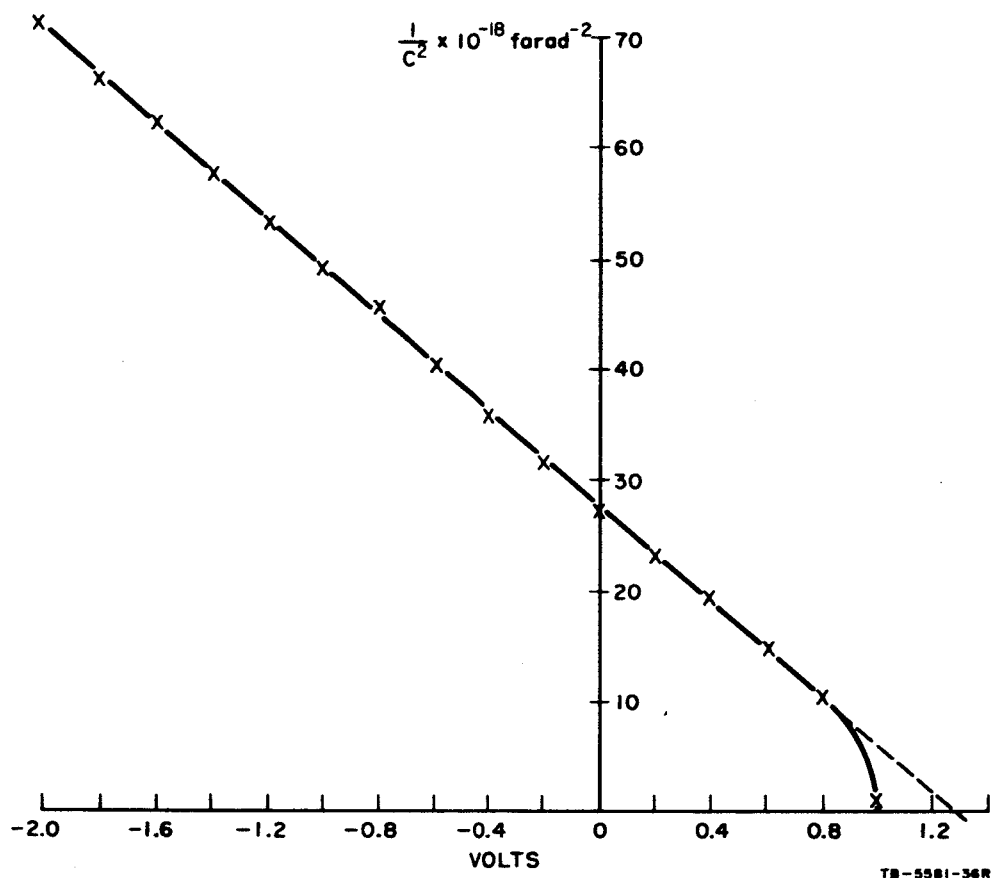


FIG. 9 PLOT OF  $1/C^2$  vs.  $V$  FOR GaP/Pd DIODE

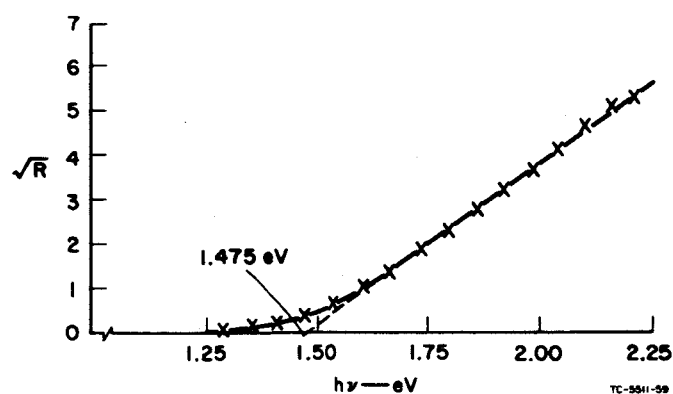


FIG. 10 SQUARE ROOT OF PHOTORESPONSE PER PHOTON vs. PHOTON ENERGY FOR GaP/Pd DIODE

It should be noted that the intercepts from all the plots of  $1/C^2$  vs.  $V$  for the GaP diodes are diffusion potentials. Assuming that the Fermi level is 0.06 eV below the conduction band, the intercept values should be increased by this amount to give the barrier height.

### C. Activation Experiments

When experimental work on BaO was started, the objective was a 1.0-eV vacuum barrier, based upon the results of Moore and Allison.<sup>6</sup> However, as the work progressed and more literature on the subject was reviewed, it became apparent that 1.0-eV photoelectric work functions were not realistic. The low values published by Moore and Allison were thermionic values, and it was found that in general the photoelectric values were a few tenths of an eV higher. Several techniques for reducing the photoelectric threshold have been reported. These include heating the substrate during the activation process, applying a field between the substrate and the BaO source during evaporation, and adding a small amount of Ba during the process. A review of some of the literature relating to these techniques was made in the Second Quarterly Report.<sup>1</sup>

#### 1. Pt/BaO

Platinum was evaporated onto a Mo substrate by inductively heating a Pt source. The freshly deposited Pt was activated with BaO in the usual manner. A shutter was incorporated in the tube to shield the substrate during the conversion of the  $BaCO_3$  to BaO. No heat was applied to the substrate during the activation process. As shown in Fig. 11, a work function of 1.60 eV was obtained in a plot of the square root of the response per photon vs. photon energy. The spectral measurement was made with the glass phototube on the vacuum station. A previous experiment in which a small amount of Pt was applied to a Ta substrate produced a double intercept. The higher value of 1.80 eV was attributed to the Pt and the lower value of 1.32 eV was associated with the Ta substrate.



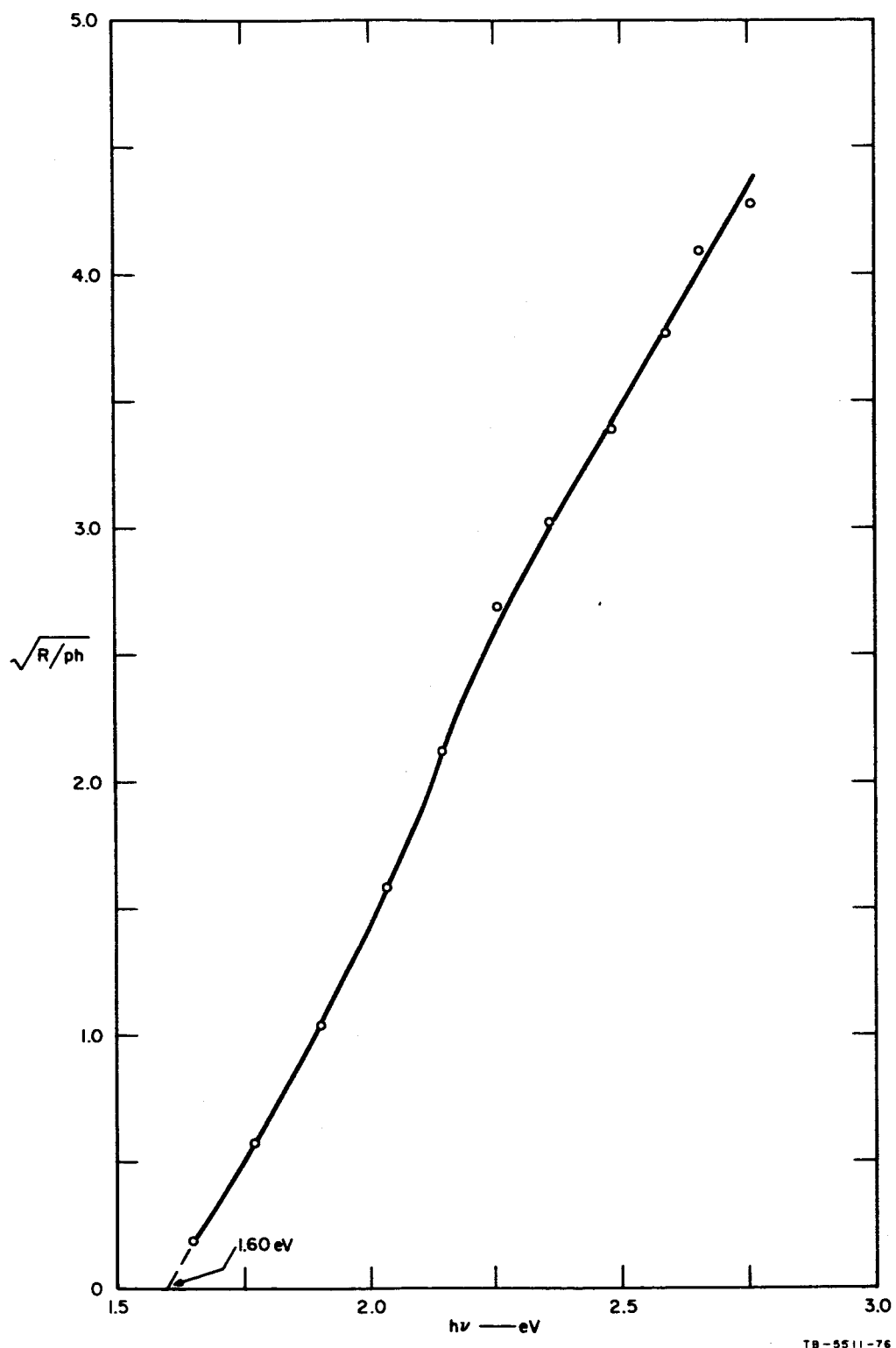


FIG. 11 SQUARE ROOT OF PHOTO RESPONSE PER PHOTON vs. PHOTON ENERGY FOR Pt/BaO PHOTOTUBE

## 2. W/BaO

A considerable amount of data was obtained on the activation of W films deposited on Mo substrates by electron beam evaporation. It was determined that the BaO film had to be 10 to 15 monolayers thick in order to obtain a uniform work function. A near-optimum value of 1.52 eV was measured with 20 to 30 monolayers as shown in Fig. 12. With less BaO the plots of the square root of the response per photon vs. photon energy were concave upwards as they approached the threshold energy. This suggests a variation in the vacuum barriers due to nonuniform BaO coverage. When more than 30 monolayers of BaO were applied, the work function increased. All these measurements were made with the photocathodes in a metal, ion-pumped system. Some deterioration in the work function with time was observed with a vacuum estimated to be  $6 \text{ to } 8 \times 10^{-9}$  torr.

## 3. Pd/BaO

Two variations in the activation process were introduced when Pd films were studied. These were a heated substrate and the addition of a small amount of Ba metal. The results were quite interesting and were reported in the Third Quarterly Report. In summary, the addition of Ba to a Pd/BaO surface with a work function of 1.7 eV reduced the value to 1.42 eV. This was carried out with the substrate at room temperature. Previous to this a threshold of 1.55 eV had been recorded with BaO alone on the Pd. The effect of the combination of heating the substrate to 600°C during the BaO evaporation and then adding Ba is shown in Fig. 13. The result of 1.45 eV is essentially the same as that obtained earlier with the substrate at room temperature. However, a double intercept obtained from a plot of the results with BaO alone on the heated substrate produced values of 1.22 eV and 1.375 eV. The lower value may have been related to the Ni substrate used in this experiment.

## 4. Ba/BaO

In reviewing the work-function values obtained by applying BaO to various metals, it appeared that the results were almost independent of the metal used. Table I summarizes these results and includes

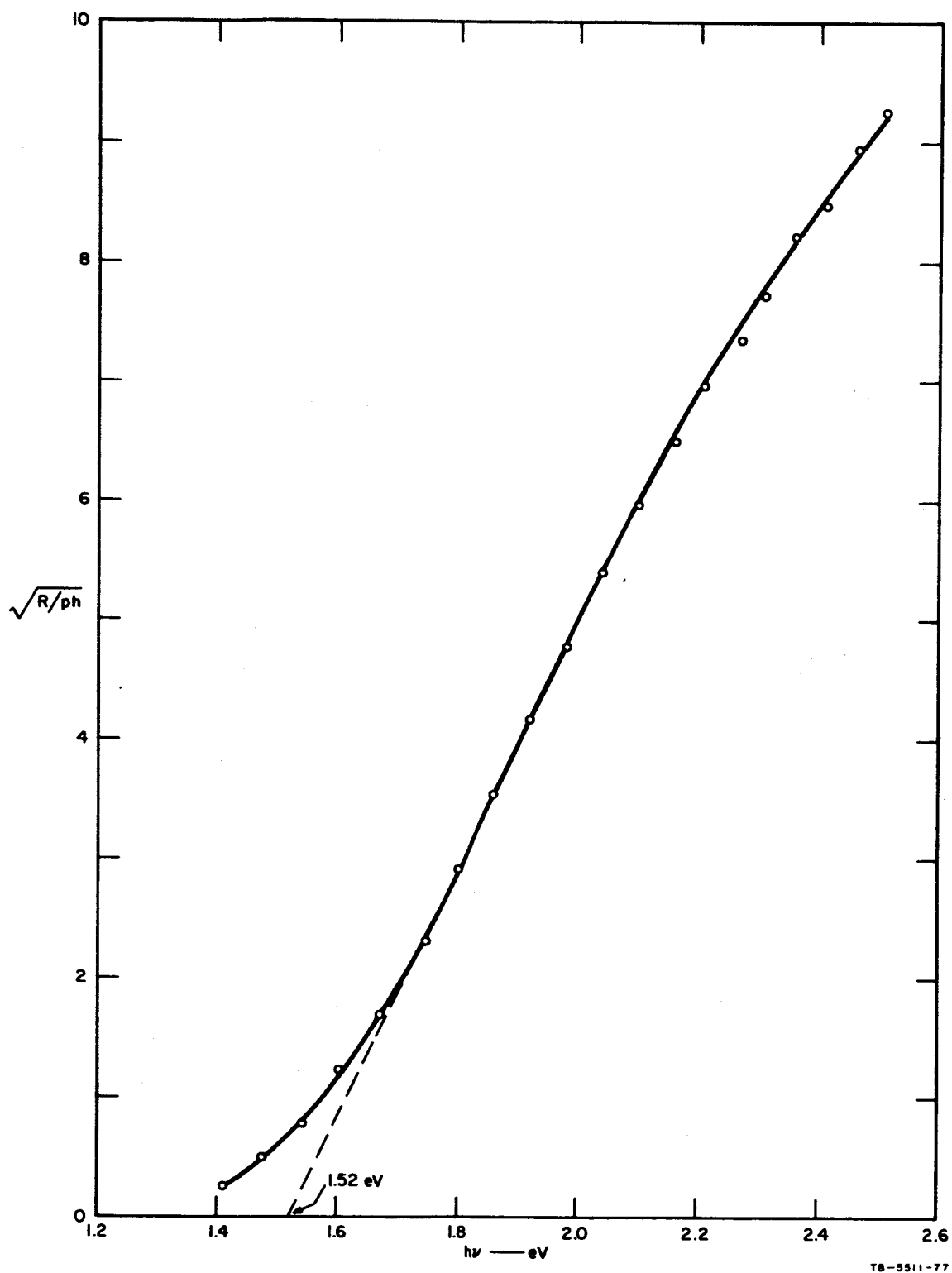


FIG. 12 SQUARE ROOT OF PHOTO RESPONSE PER PHOTON vs. PHOTON ENERGY FOR W/BaO PHOTOTUBE

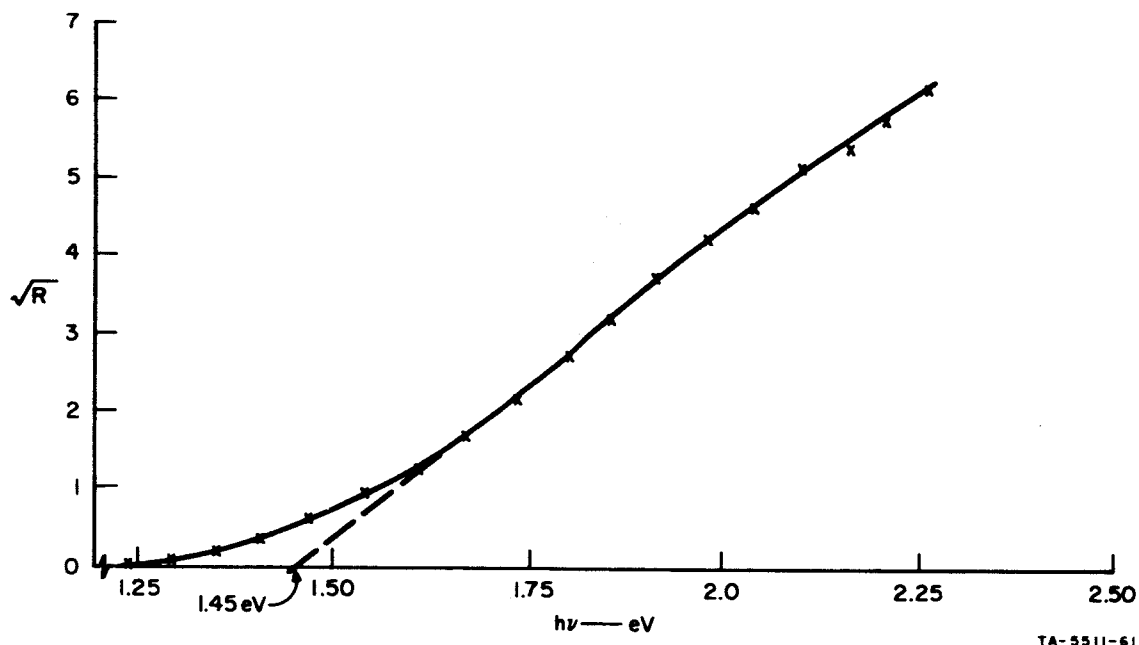


FIG. 13 SQUARE ROOT OF PHOTORESPONSE PER PHOTON vs. PHOTON ENERGY FOR Pd/BaO/Ba SURFACE (BaO deposited on heated substrate)

the ratio of the final work function to the initial work function as well as the difference in these values. It was decided to try activating a Ba metal film with BaO to determine the effect of starting with a low-work-function metal. The result is shown in Fig. 14, which has an intercept of 1.48 eV. Although other factors may be involved, it seems that the initial work function of the metal has little effect on the activation process.

##### 5. Ni/BaO

Some results on Ni were included in the Third Quarterly Report.<sup>5</sup> In the last quarter of this program more measurements were made on Ni/BaO cathodes which were formed by depositing BaO on Ni at 600°C. Figure 15 is a plot of the photoresponse and the thermionic emission as a function of temperature. It was found that the thermionic component could be reduced with negligible effect on the photoelectric component by reducing the anode potential (Fig. 16).

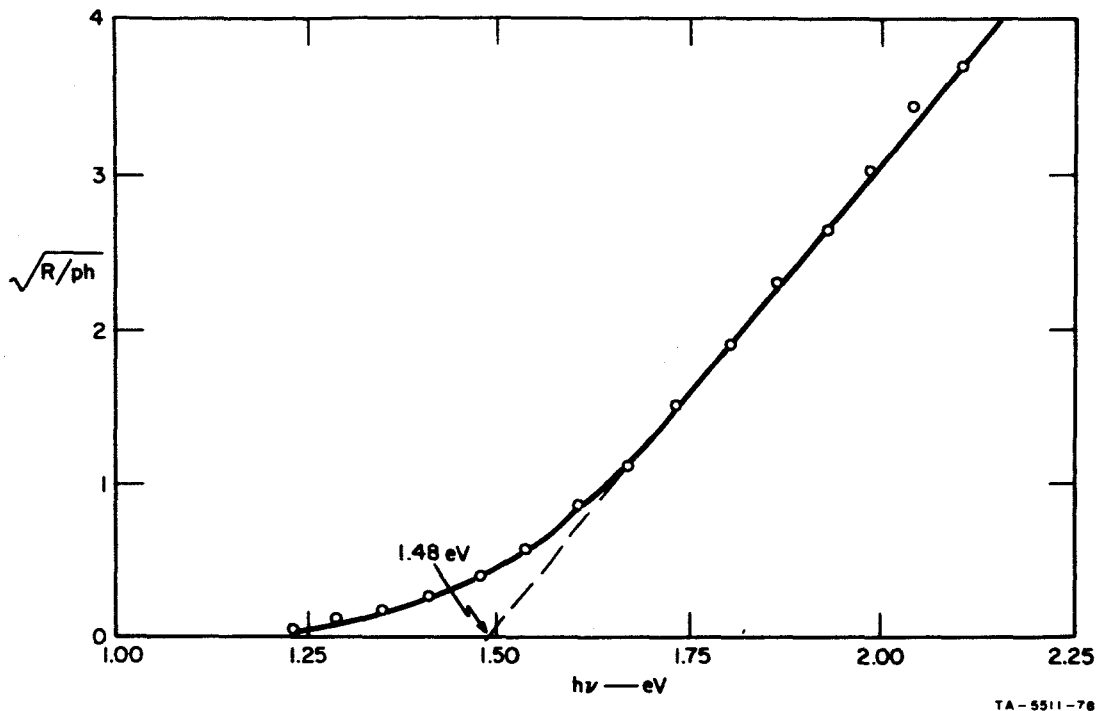


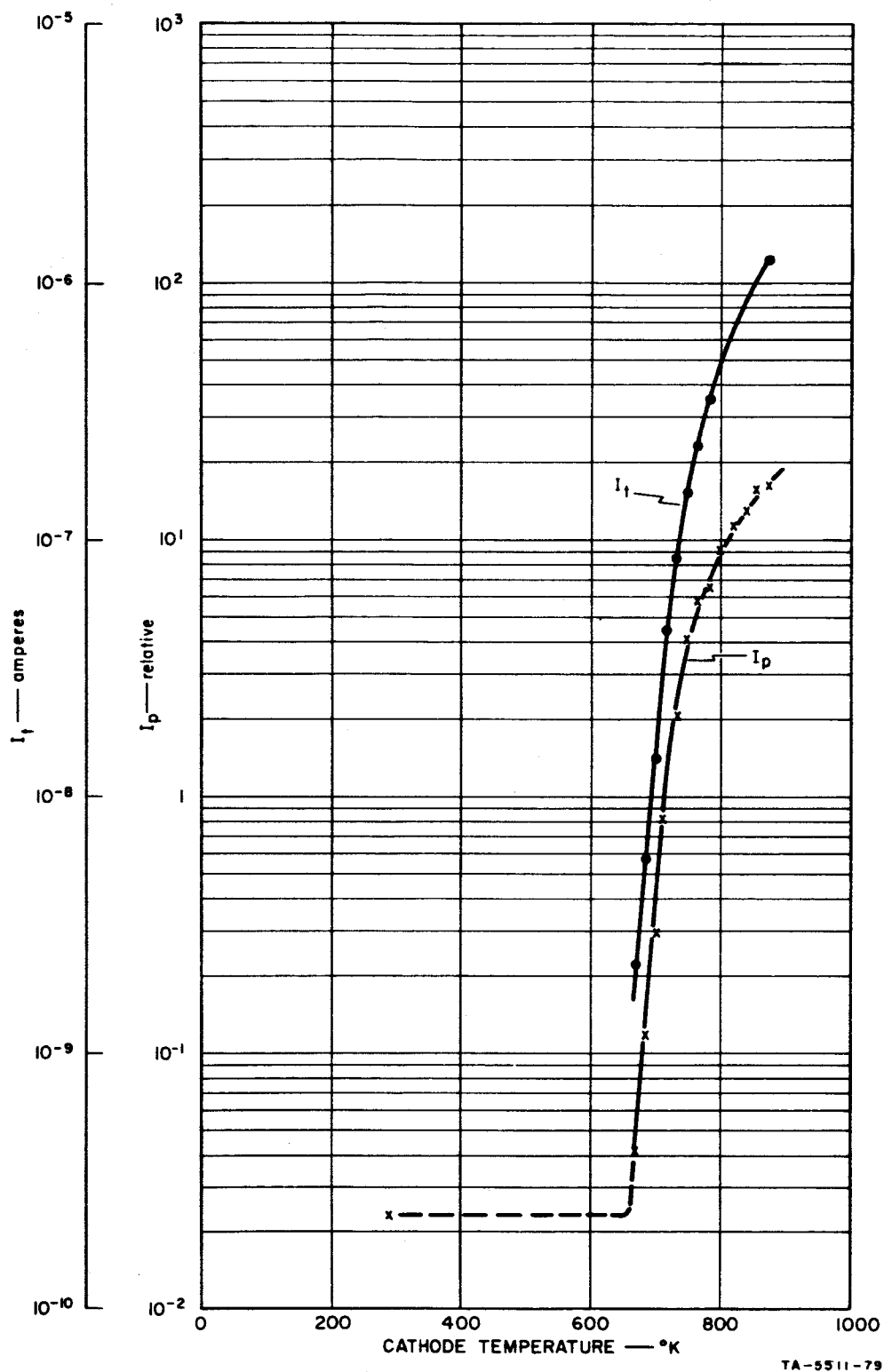
FIG. 14 SQUARE ROOT OF PHOTORESPONSE PER PHOTON vs. PHOTON ENERGY FOR Ba/BaO PHOTOTUBE

The spectral response at approximately 600°C is interesting because of the unusual low energy "tail" shown in Fig. 17. It was also observed that the sensitivity at higher photon energies was greatly enhanced by operating the cathode at this elevated temperature. A plot of the increase in photocurrent due to Fowler theory (see Appendix A of the First Quarterly Report<sup>2</sup>) is given in Fig. 18 along with the observed photoresponse. The current predicted by the Fowler theory is about two orders of magnitude below the measured values. Other mechanisms to explain this effect are being considered in order to obtain a better understanding of the BaO activation process.

#### D. Alternate Cathode Structures

##### 1. Transistor Cathode

The concept of the transistor cathode was described in the Third Quarterly Report.<sup>5</sup> Energy diagrams with and without bias are



TA-5511-79

FIG. 15 PHOTORESPONSE AND THERMIONIC EMISSION AS A FUNCTION OF TEMPERATURE FOR Ni/BaO CATHODE (BaO deposited on Ni at 600°C)

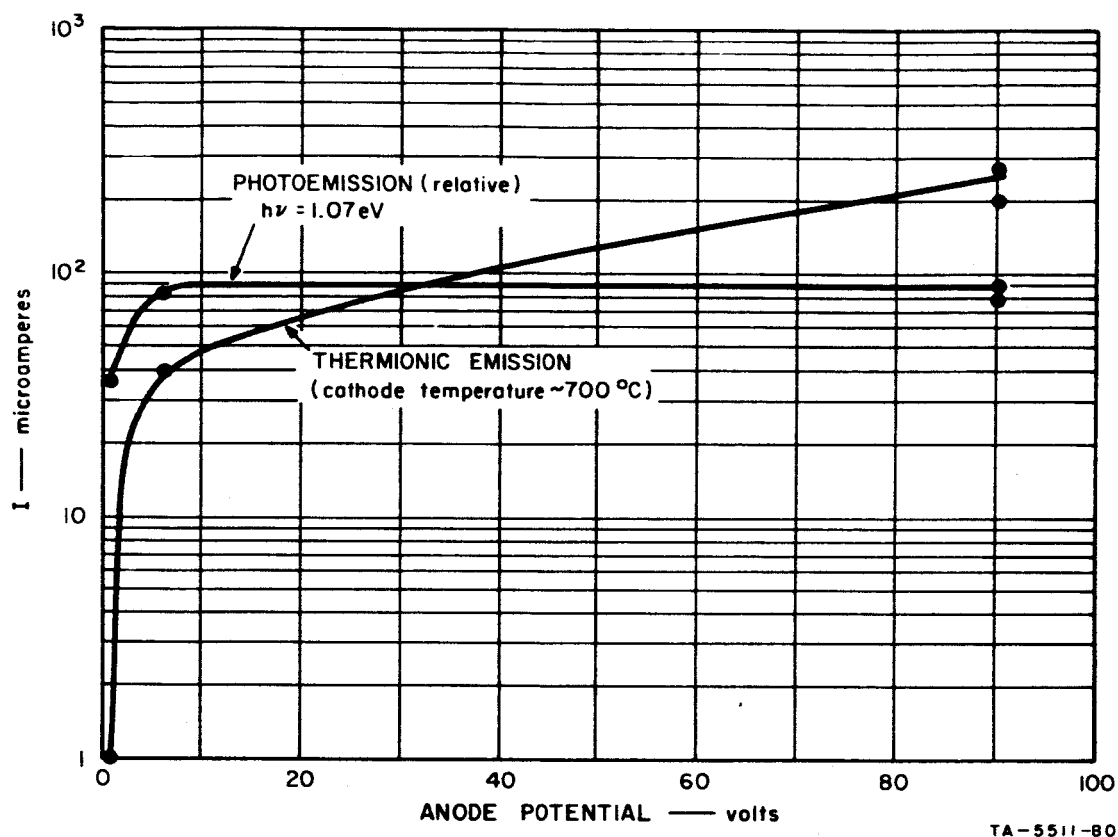


FIG. 16 PHOTOELECTRIC AND THERMIONIC EMISSION COMPONENTS AS A FUNCTION OF ANODE VOLTAGE FOR Ni/BaO CATHODE (BaO deposited on Ni at 600°C)

reproduced in Fig. 19. The operation of the cathode resembles that of an n-p-n transistor, with the vacuum replacing the collector. One of the attractive features of this cathode is the absence of the thin metal surface film required in the surface-barrier cathode. However, it does require a surface treatment to produce a low vacuum barrier. Some experimental work along these lines has been performed by exposing freshly cleaved GaAs crystals to BaO. One of the objectives in this work was to determine if results similar to those of Scheer and van Laar<sup>7</sup> could be obtained by using BaO in place of cesium on GaAs.

In the first experiment the GaAs cleaved very nicely during the evaporation of BaO from a nickel cathode structure, which was held at a temperature of approximately 1070°C. After 2 minutes of evaporation the spectral response of the cathode was measured to determine the photosensitivity and the photothreshold. The sensitivity was rather

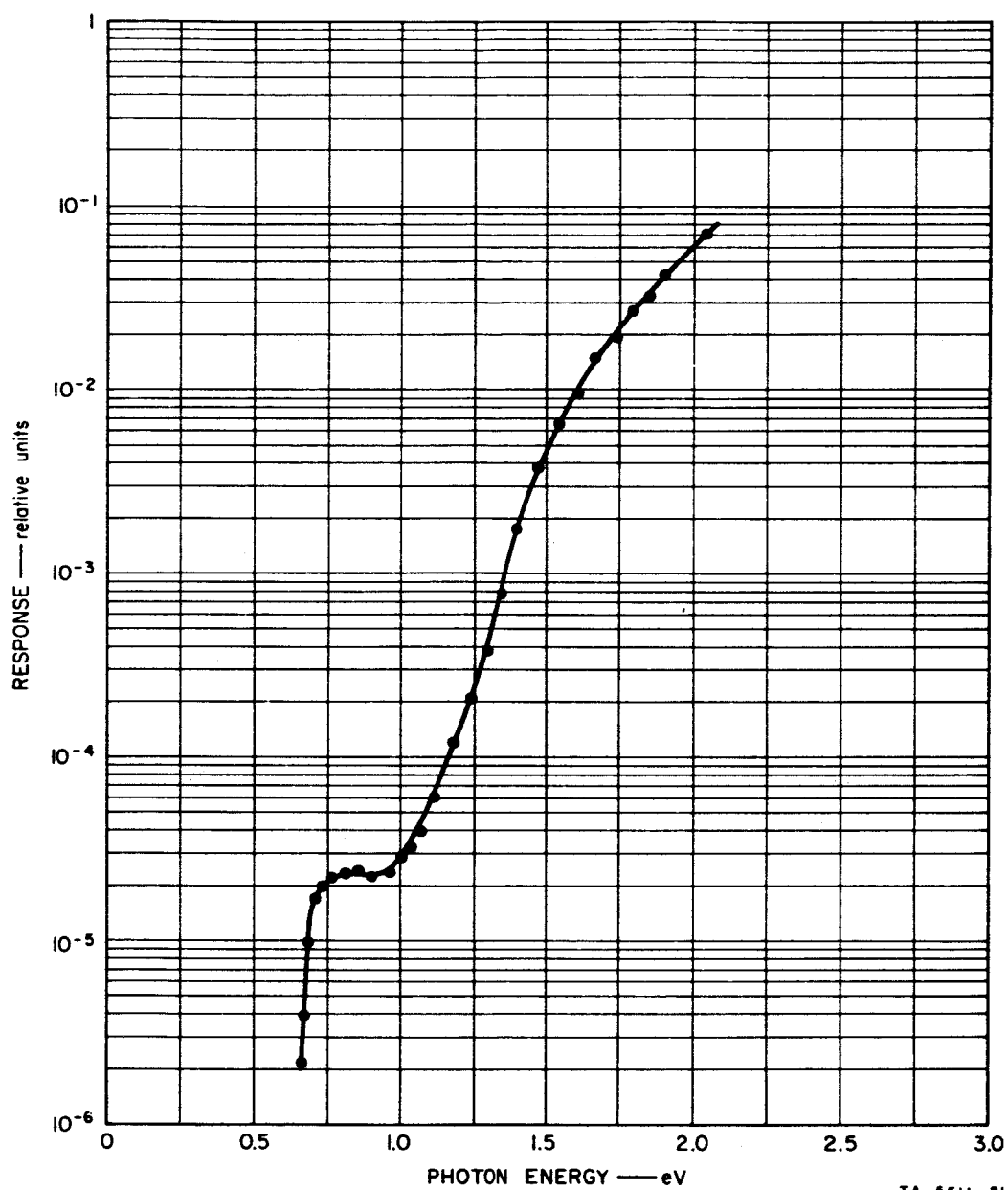


FIG. 17 SPECTRAL RESPONSE OF Ni/BaO CATHODE AT APPROXIMATELY 600°C  
(BaO deposited on Ni at 600°C)

poor but the threshold had been brought down from that of bulk GaAs to about 1.67 eV. The response is shown in Fig. 20. In order to improve the sensitivity, BaO was evaporated for an additional minute at 1070°C, which resulted in less sensitivity and a threshold of 1.80 eV. BaO was evaporated for one more minute at a source temperature of 1000°C, which



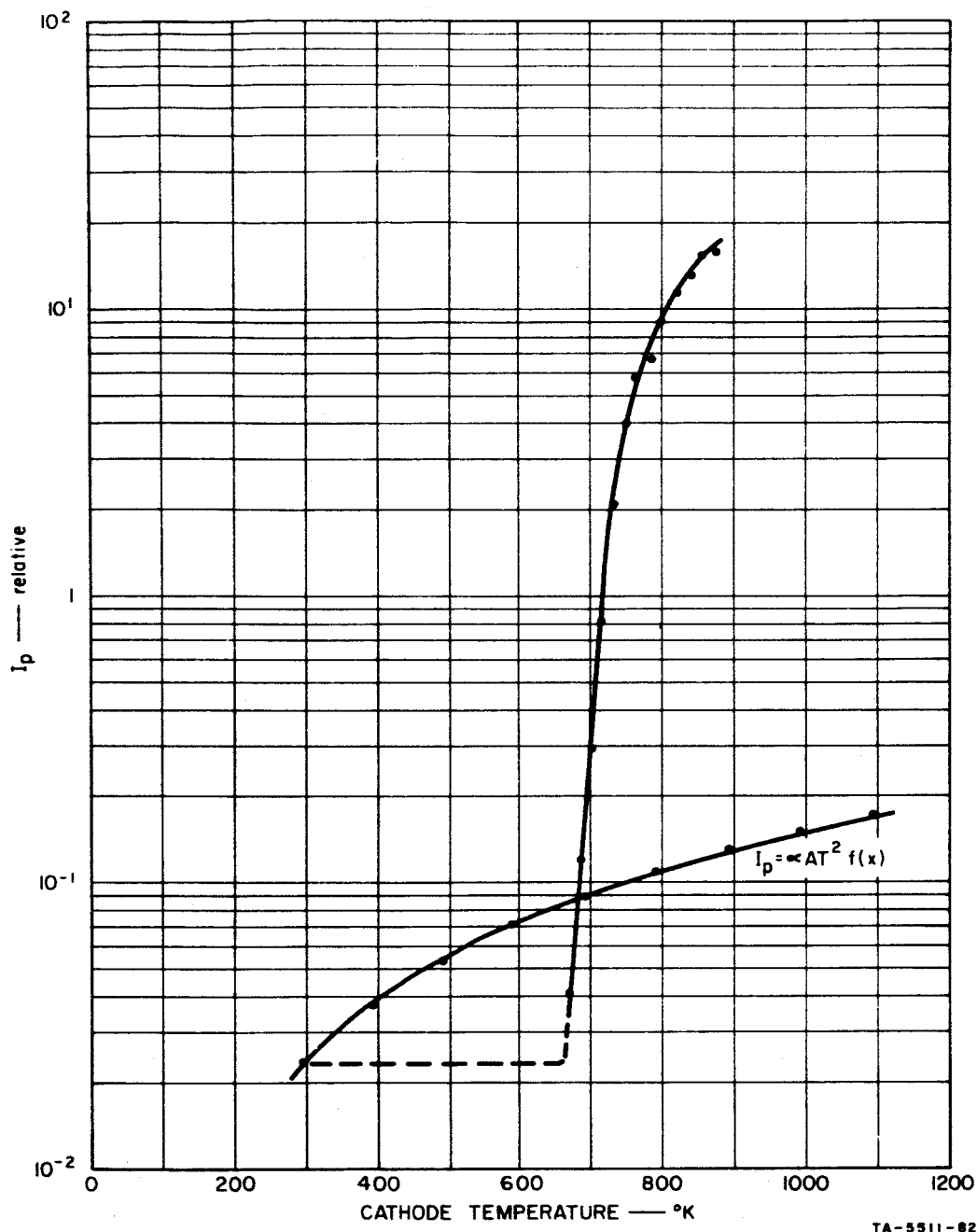
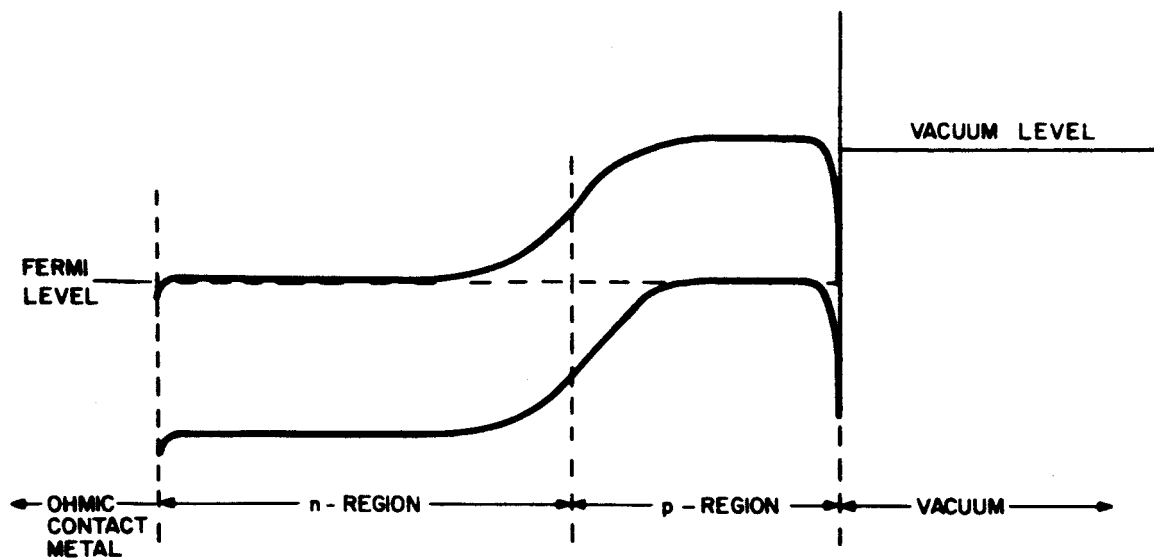
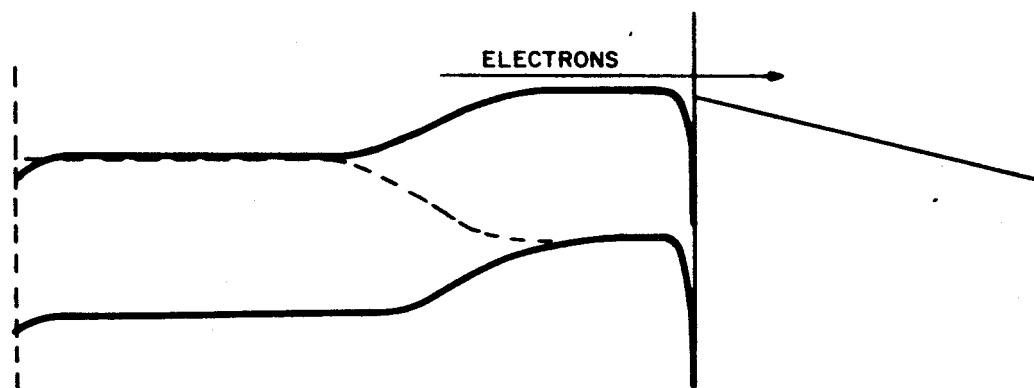


FIG. 18 OBSERVED PHOTORESPONSE AND CURRENT PREDICTED FROM FOWLER ANALYSIS AS A FUNCTION OF TEMPERATURE FOR Ni/BaO CATHODE

resulted in even lower sensitivity and a higher threshold energy. Thus, it was obvious that the optimum thickness of BaO had been exceeded and this experiment was terminated.



(a) WITH NO BIAS VOLTAGE APPLIED.



(b) WITH BIAS VOLTAGE APPLIED.

TA-5511-51

FIG. 19 ENERGY DIAGRAMS FOR TRANSISTOR CATHODE

The second experiment was set up in exactly the same manner as the first but the second crystal did not cleave as well as in the first experiment. The BaO evaporation temperature was further reduced to  $950^{\circ}\text{C}$  and the sensitivity was checked at 1/2-minute intervals to determine the optimum thickness of BaO. Good control was obtained using this procedure, and the thickness of the BaO was optimized. The best sensitivity and lowest-threshold energy coincided, as would be expected. Beyond the optimum amount of BaO the sensitivity decreased about as rapidly

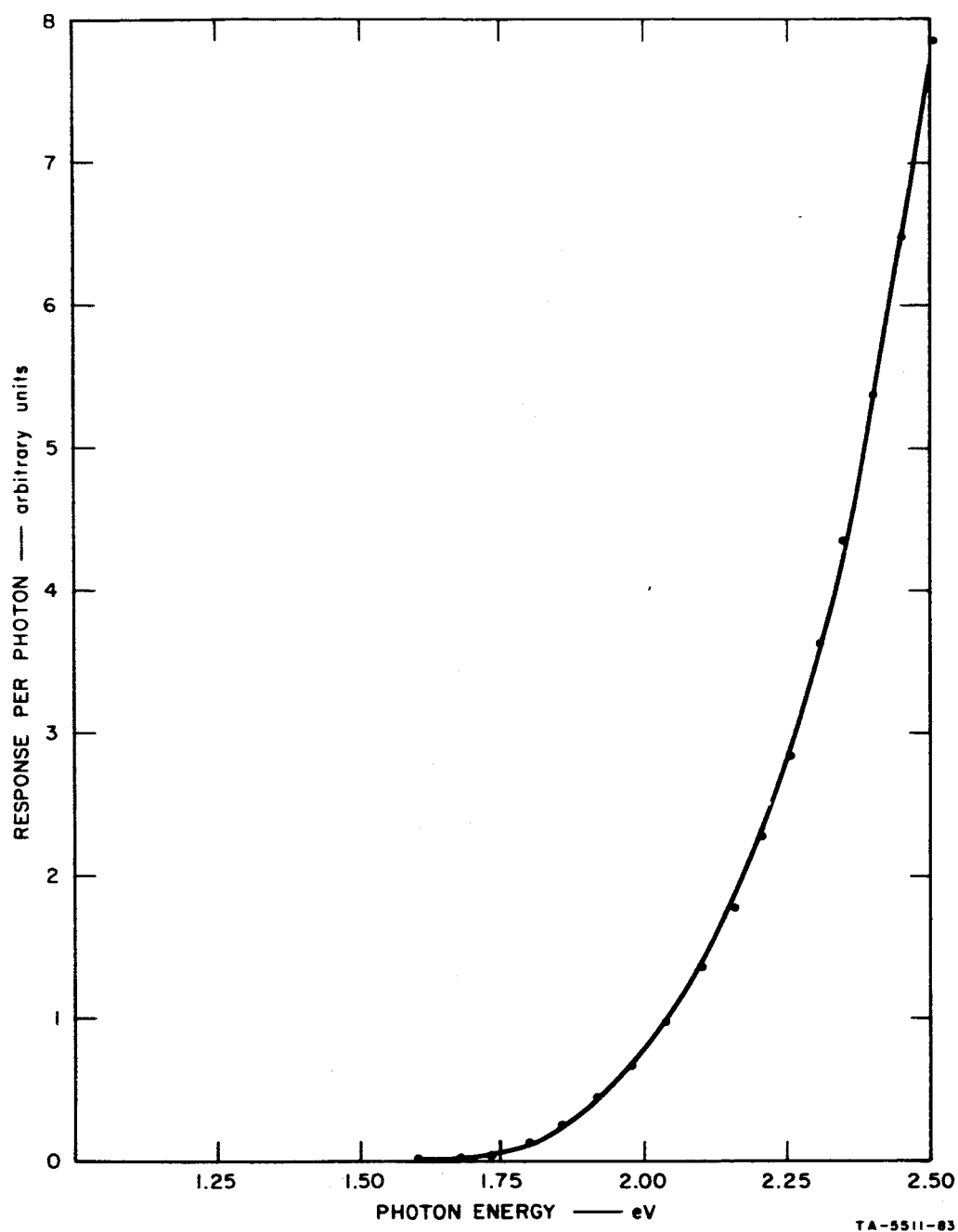


FIG. 20 RESPONSE PER PHOTON vs. PHOTON ENERGY FOR BaO-ACTIVATED GaAs

as it had increased, while the threshold energy increased at a much slower rate. The cathode was found to be unstable, decreasing in sensitivity to about 60% of its original value in about 4 hours. The cathode

could be brought back to its original sensitivity and work function with the evaporation of more BaO. If less than an optimum amount of BaO was applied, the cathode sensitivity simply decreased with time. If too much BaO was put on, the sensitivity would increase through a peak and then decrease, as shown in Fig. 21.

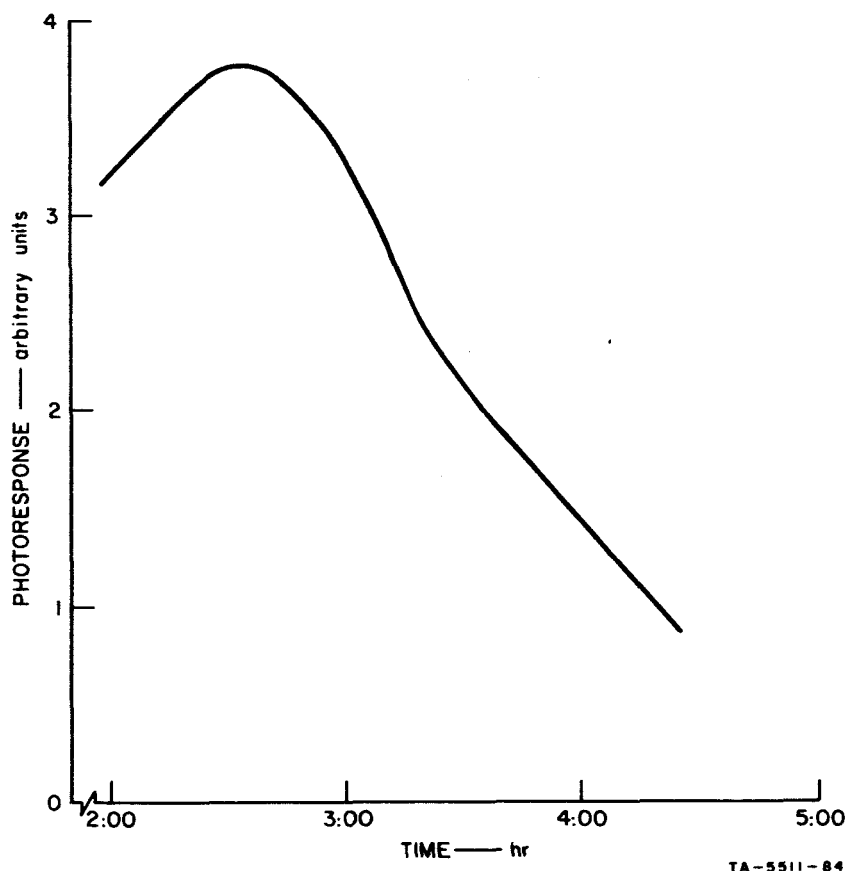


FIG. 21 VARIATION IN RESPONSE OF BaO-ACTIVATED GaAs CRYSTAL AS A FUNCTION OF TIME

Photoemission from the cathode decreased to negligible values in a 12-hour period. After this decrease, the cathode could be reactivated to its initial sensitivity and work function by the application of more BaO. The same schedule of evaporation and testing was followed on the second day, using a source temperature of 950°C and 1/2-minute

evaporations of BaO. The cathode activated more rapidly than on the first day but followed the same pattern of decay. It is uncertain at this point whether the decay was caused by the BaO leaving the surface or a layer of contamination was building up on the surface.

In the next experiment the GaAs crystal was heated to a temperature of 400°C during the application of BaO. Thresholds as low as 1.25 eV were obtained in spectral response measurements, but the sensitivity was very low. In consulting with Prof. W. Spicer from Stanford University, it was suggested that most of the response was coming from the BaO, not from the GaAs. The mobility of the GaAs was not particularly high and due to the low absorption characteristics of the material, the carriers with enough energy to escape into vacuum were generated so deep in the GaAs that they lost their energy before reaching the surface. It is planned to carry out further experiments with higher mobility and heavier doped GaAs.

## 2. The Transverse Field Cathode

One of the earliest incidences of hot electron emission reported is the emission from back-biased Si P-N junctions.<sup>8</sup> The emission occurred along the line of the exposed junction where it intersected the surface. This type of emitter suffers from two serious drawbacks. For one thing, most of the current through the junctions is completely wasted because of the very poor geometry of the device. Attempts have been made to obtain broad-area emission from a face of the n-type region parallel and very close to the junction, but these attempts have apparently not been too successful. For another thing, Si is a poor material to use for such a transverse-field emitter because of its small bandgap. The threshold for pair production is only about 2 volts above the bottom of the conduction band, making it exceedingly difficult to obtain hot electrons above the vacuum energy level. Most workers have attempted to overcome this limitation by cesiating the surface in order to bring the vacuum energy level down below the threshold for pair production.

The drawbacks of the P-N junction Si hot-electron emitter can be overcome through proper design and by using appropriate materials. First of all, the very large current losses through the P-N junction can be reduced orders of magnitude by using evaporated metal electrodes on a face of a suitable semiconductor or insulator crystal as shown in Fig. 22. In this arrangement, most of the current flows very close to the

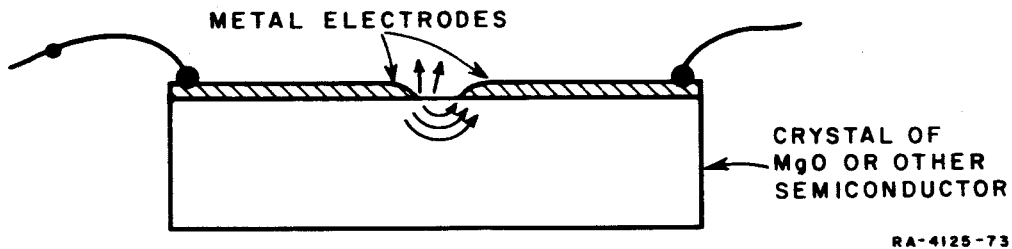


FIG. 22 SCHEMATIC DRAWING OF M-I TRANSVERSE FIELD EMITTER

face of the crystal where it is exposed to the vacuum in the gap between the two metallic electrodes. The gap between the two metal films should be narrow enough so that high electric fields can be created by low applied dc potentials--for example, 10 volts. Fields of  $10^3$  to  $10^4$  volts/cm should be sufficient to generate appreciable quantities of hot electrons, and a narrow gap ensures that the majority of the current flow occurs very near to the exposed surface of the crystal.

An alternative arrangement is shown in Fig. 23. In this case the metal electrodes are evaporated onto a very good dielectric having a high breakdown strength, such as quartz. Then a thin layer of a suitable semiconductor or semi-insulator is deposited over the metals, as shown. This arrangement has the advantage over the single-crystal scheme shown in Fig. 22, that all of the current can be made to flow very close to the surface of the top layer, yielding improved efficiency.

An ideal semiconductor for the transverse-field semiconductor emitter would have the following properties:

- (1) A large bandgap, so that the threshold energy for pair production would be high

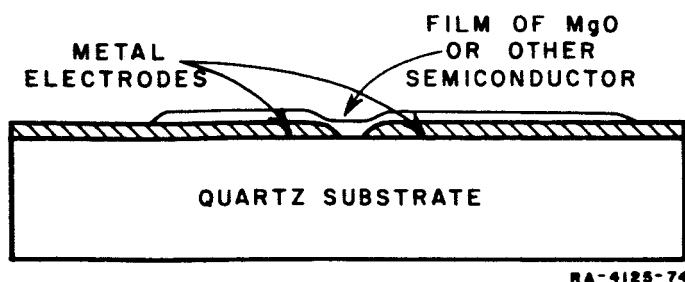


FIG. 23 SCHEMATIC DRAWING OF ALTERNATIVE  
TRANSVERSE FIELD SEMICONDUCTOR EMITTER

- (2) A low electron affinity, so that a large percentage of the hot electrons could escape into the vacuum at relatively low values of electric field without requiring a low-work-function treatment
- (3) A low vapor pressure and a high melting point
- (4) Good chemical stability and inertness.

The theory of the transverse-field semiconductor emitter is straight-forward. Electrons are simply accelerated to high energy levels by a strong field existing across a narrow region of the material, and because of electron-phonon interactions the momentum of the electrons is randomized. Thus, many of the hot electrons obtain momentum perpendicular to the surface, and sufficient energy is associated with the momentum for the electron to overcome the work function at the surface and escape into the vacuum. Then, provided an accelerating field is presented to the electrons by a positively biased electrode near the surface, the electrons can be accelerated into the vacuum and used as desired.

During emission tests on  $\text{TiO}_2$  cathode structures in a previous study for Microwave Electronics Corporation, a transverse-field mode of operation was obtained. This was due to fissures developing in molybdenum surface films and subsequent exposure to  $\text{BaO}$ . A deliberate experiment to demonstrate the capabilities of this type of emitter was performed in the last quarter of the current program. The technique and the results obtained are described in Sec. II-E-2 of this report.

## E. Emission Tests

### 1. GaP/Pd/BaO Cathodes

Experiments with GaP/Pd cathode structures activated with BaO were described in the Third Quarterly Report.<sup>5</sup> Reasonable diode characteristics were obtained prior to assembly and processing for emission. The GaP/Pd barrier heights were of the same order measured previously (Sec. II-B-3), but there was only a small margin between this value and attainable Pd/BaO vacuum barriers. When the GaP/Pd barrier deteriorated during a bake-out cycle, this margin was lost.

It is possible that surface states due to defects at the GaP/Pd interface pushed the barrier up, and when some of these defects were annealed out, the barrier came down. Another factor being considered is a distribution of barrier heights (Appendix A, Third Quarterly Report).<sup>5</sup> When bias is applied, the current in the low barrier regions dominates, and very few electrons acquire enough energy to escape into the vacuum.

### 2. Si/BaO/Al Transverse Field Cathode

A relatively simple structure was used to demonstrate the concept of the transverse field cathode. A wafer of low-resistivity silicon was oxidized thermally to produce about one micron of  $\text{SiO}_2$  on its surface. A film of Al was then evaporated on top of the oxide on one side and the wafer was cleaved into smaller sections having well defined edges. After etching off the oxide on the reverse side, one of these sections was bonded to a standard TO-9 gold-plated header. This was mounted in a glass envelope with a tungsten wire probe making contact to the Al film. A BaO source was mounted so that BaO would evaporate onto the exposed edge of the structure (Fig. 24). A sliding shutter between the BaO source and the structure was included to prevent contamination during the conversion of the  $\text{BaCO}_3$  to the oxide. This shutter later served as an effective collector during the emission measurements.

Processing included an overnight bake-out at  $300^\circ\text{C}$ , followed by conversion of the carbonate and another overnight bake-out. Barium



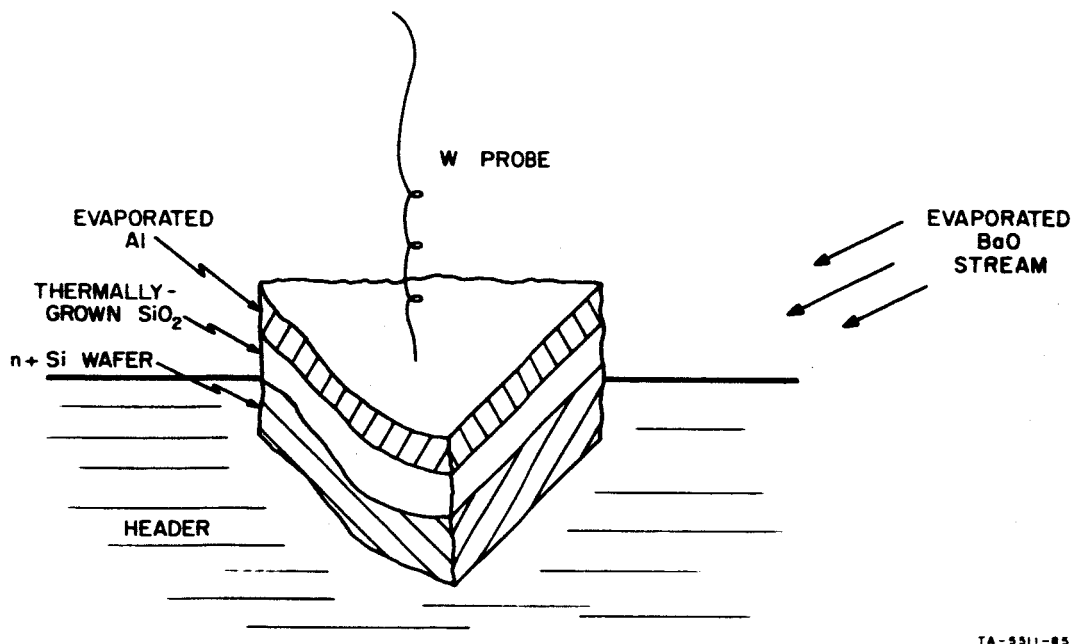


FIG. 24 EXPERIMENTAL TRANSVERSE-FIELD COLD-CATHODE STRUCTURE

getters were fired and the tube was tipped off. A 100V bias supply was connected across the  $\text{SiO}_2$  layer and BaO evaporated until a bias current of a few microamperes was obtained between the aluminum film and the silicon.

A considerable amount of emission data was obtained from this tube. Figures 25(a), (b), and (c) show plots of bias current and collector current vs. bias voltage for collector potentials of 300, 600, and 900 volts, respectively. More BaO was evaporated after the measurements were taken with 300V on the collector, and from the ratios of  $I_c/I_b$  it appears that the cathode was less efficient with the additional BaO. Initially this ratio was greater than 0.10 at higher bias voltages, and values as high as 0.46 were recorded.

Using a collector current of 10  $\mu\text{A}$  from Fig. 25(c), an emission current density of 1/3 ampere per square cm is obtained for the edge nearest to the BaO source. The contribution to the current from the other edges is not known, but from the geometry used it should be quite small. The cathode was operated for several hours at one microampere of collector current. There was some instability, but undoubtedly this

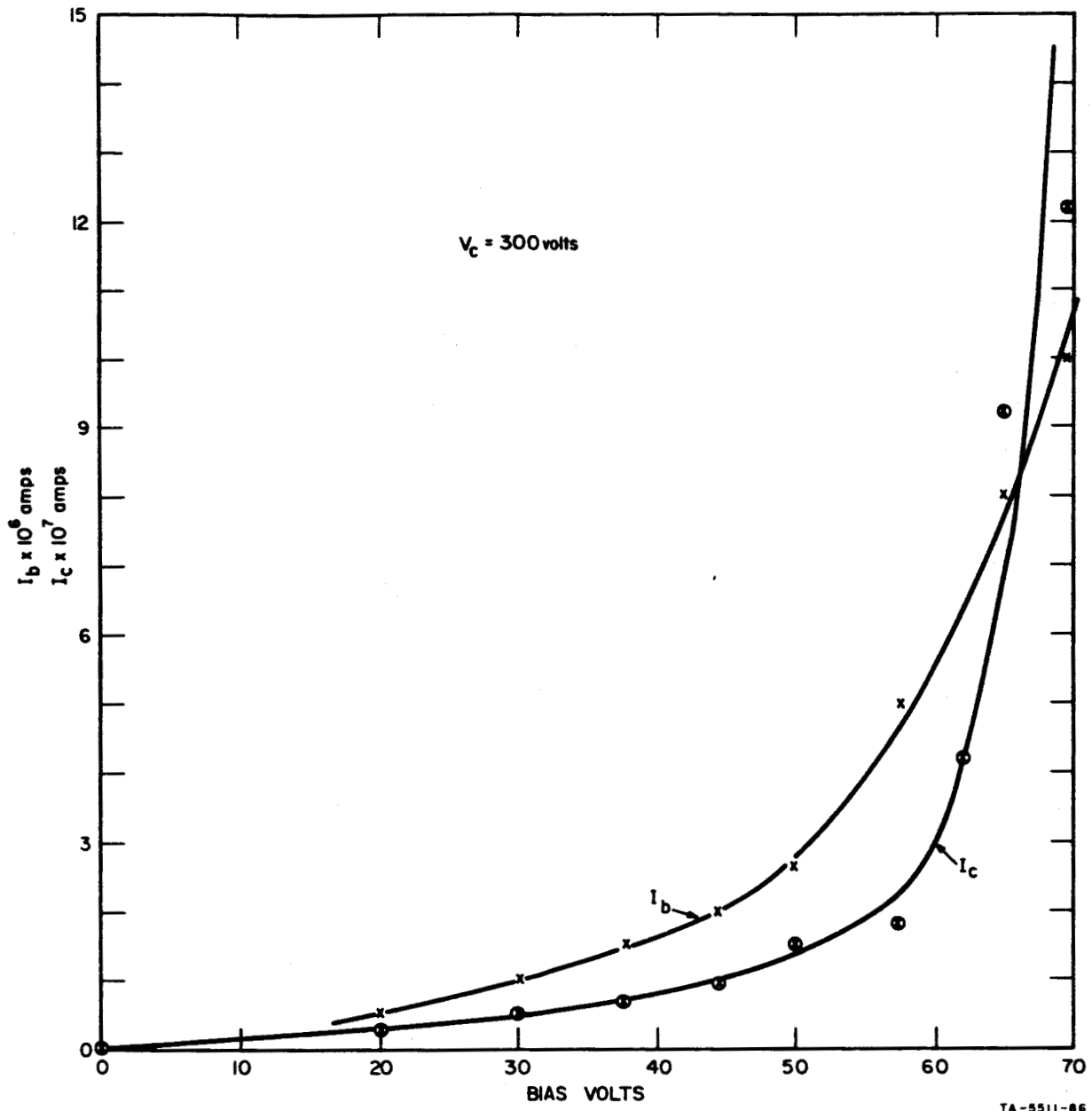


FIG. 25(a) PLOT OF BIAS CURRENT AND COLLECTOR CURRENT vs. BIAS VOLTAGE FOR TRANSVERSE-FIELD EMITTER (Collector Voltage = 300V)

could be improved by increasing the emitting area and operating at lower current densities.

Figure 26 is a plot of collector current vs. collector voltage at a constant bias current of 30  $\mu$ A. At collector voltages below 350V

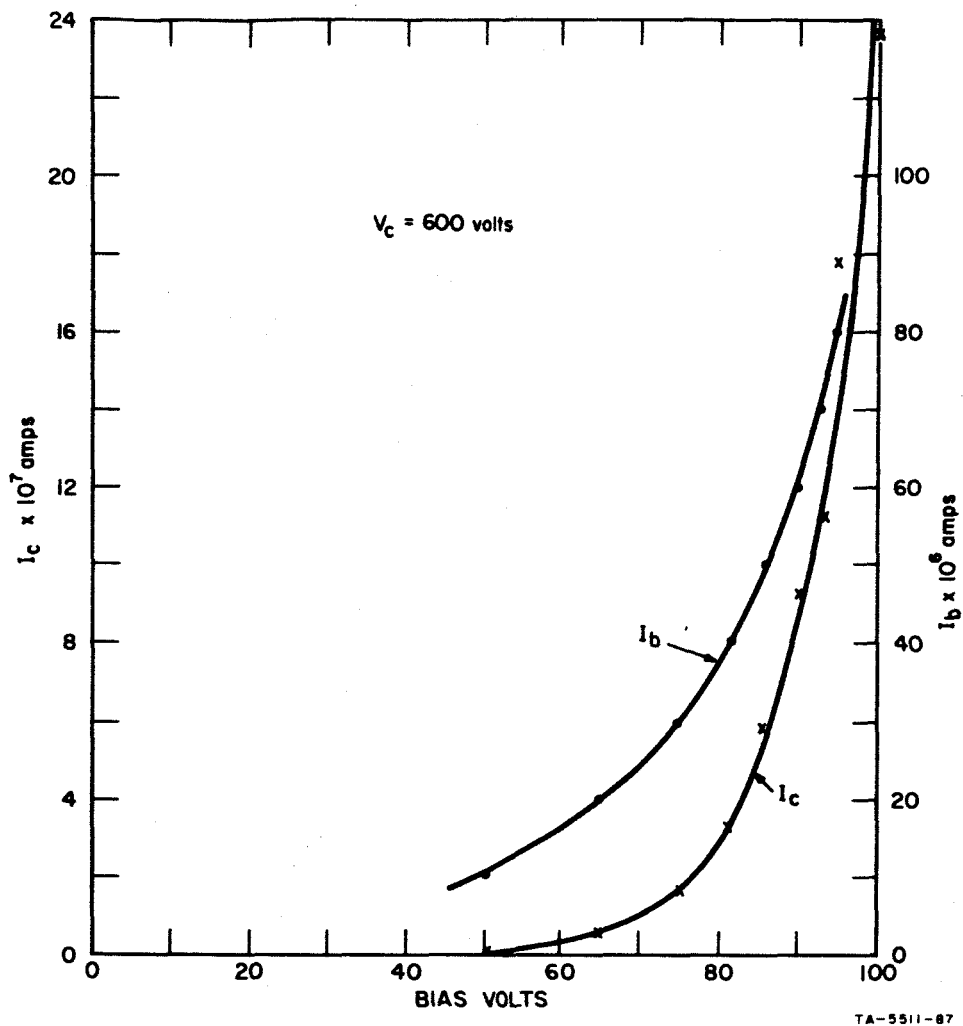


FIG. 25(b) PLOT OF BIAS CURRENT AND COLLECTOR CURRENT vs. BIAS VOLTAGE FOR TRANSVERSE-FIELD EMITTER (Collector Voltage = 600V)

the current may be space-charge limited. At higher collector voltages there is some indication of saturation or transverse field-limited emission. This is consistent with the characteristics predicted for this type of emitter.

#### F. Life Tests

##### 1. GaP/Pt Diode

One diode of this type was operated for 4300 hours at 1.5V applied bias with no apparent change in its characteristics during this

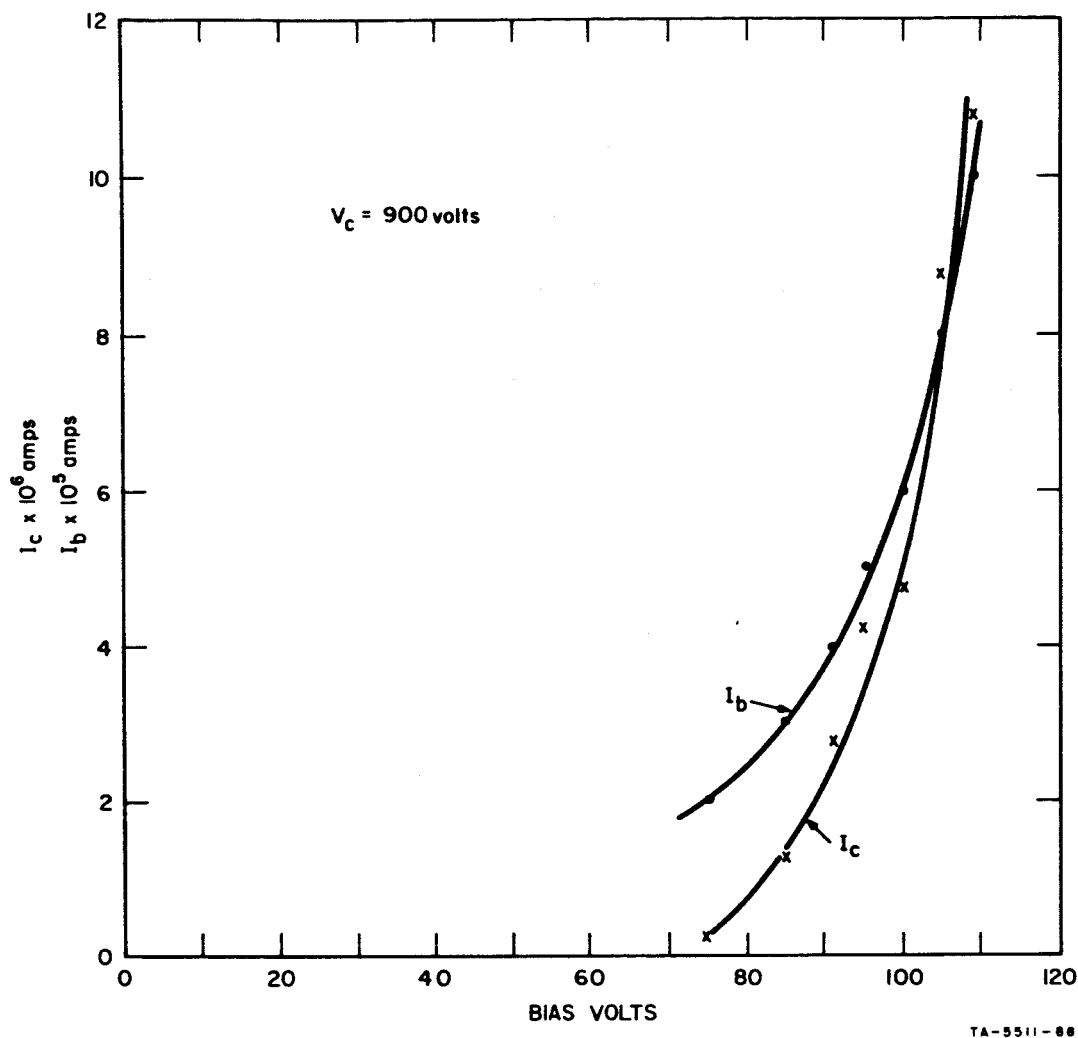


FIG. 25(c) PLOT OF BIAS CURRENT AND COLLECTOR CURRENT vs. BIAS VOLTAGE FOR TRANSVERSE-FIELD EMITTER (Collector Voltage = 900V)

period. The test was terminated when the probe contact to the Pt film became intermittent. A second diode on the same GaP crystal was then placed on test. After 1500 hours of operation at 1.0V applied bias, the I-V characteristic became "soft." The test on the original diode was then resumed and it has been operating for an additional 2000 hours at 1.5V bias.

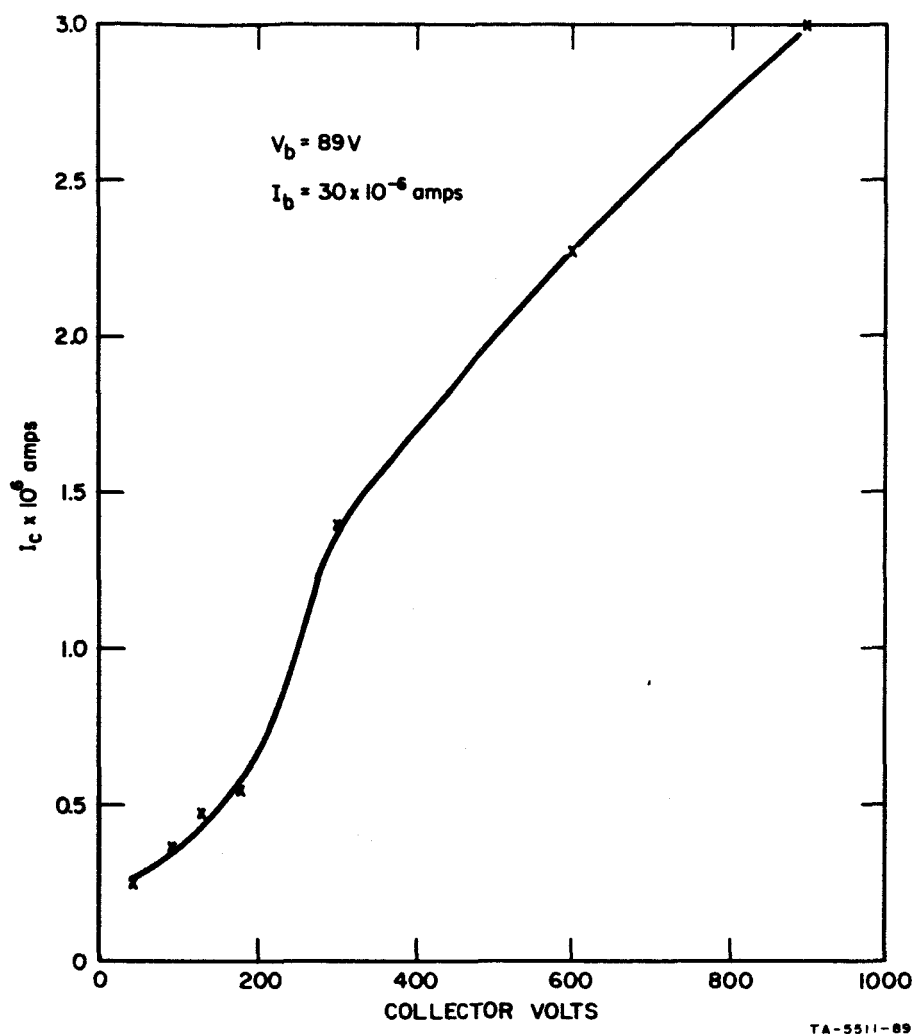


FIG. 26 PLOT OF COLLECTOR CURRENT vs. COLLECTOR VOLTAGE FOR TRANSVERSE-FIELD EMITTER (Bias Voltage = 89V, Bias Current =  $30 \mu A$ )

## 2. GaP/Pd Diode

The GaP/Pd diode has an accumulated life of almost 2000 hours at 1.0V forward bias. Figure 27 is a photograph of the I-V characteristic on a curve tracer. The test was interrupted for two weeks while other measurements were made on the diode.

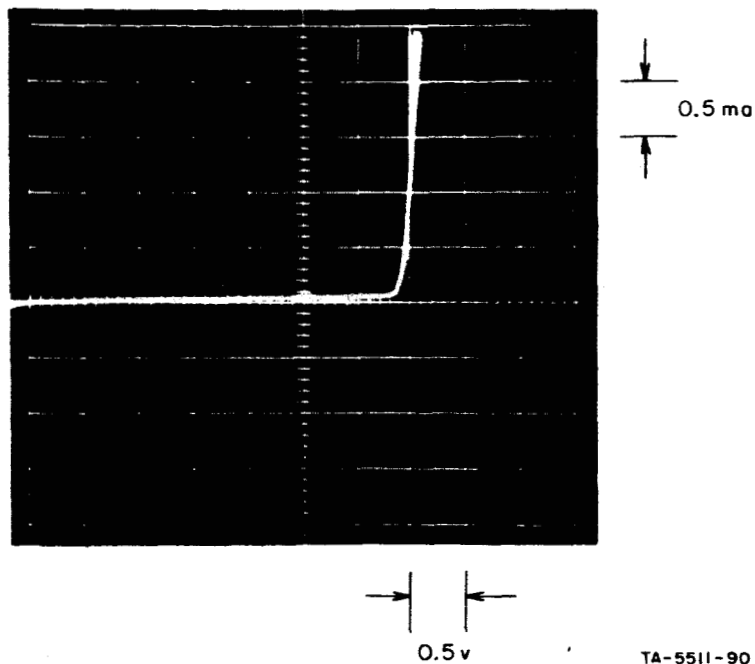


FIG. 27 PHOTOGRAPH OF I-V CHARACTERISTICS OF GaP/Pd DIODE ON LIFE TEST

### 3. Ag/BaO Phototube

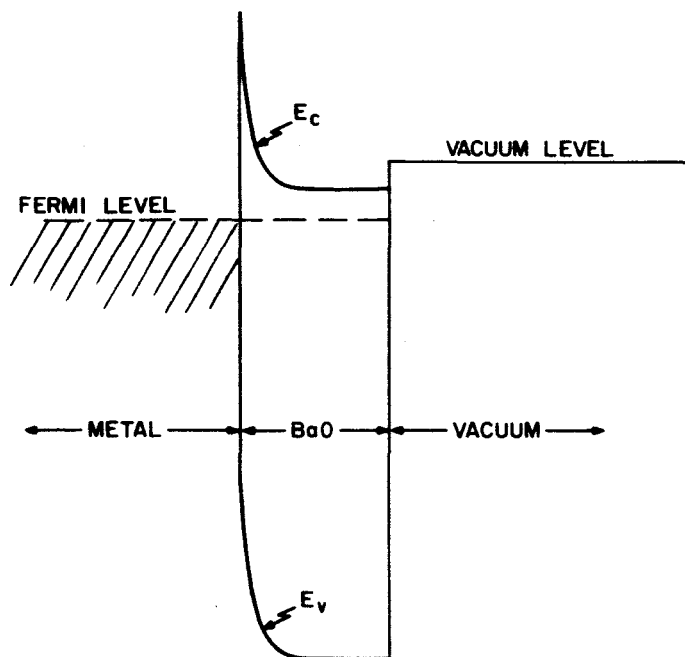
The most recent measurement on an Ag/BaO phototube with a total shelf life of 14,000 hours is 1.55 eV. The results of six previous measurements over a period of 16 months have been reported.<sup>5</sup> The average of all measurements to date is 1.49 eV.

### III CONCLUSIONS

#### A. Surface-Barrier Cathode

A surface-barrier cathode using GaP for the semiconductor and BaO for the activator does not appear to be a workable combination. Several explanations and combinations of conditions could be responsible. First of all, the GaP/metal diodes fabricated and tested to date do not follow Schottky theory. Thus the exact mechanism of current flow is not known. Under forward bias, the GaP may not be injecting hot electrons into the metal. An interfacial contaminating layer between the GaP and the metal could be causing severe electron losses before the electrons reach the metal. Second, there are several indications that the GaP/metal diodes fabricated and tested to date do not have uniform barriers. Plots of  $1/C^2$  vs.  $V$ , spectral response, and  $J$  vs.  $V$  all indicate that the barriers are nonuniform, with barrier regions below one eV. Thus, most of the current flow could be over the low barrier regions. Third, even a mild bake-out ( $\sim 200^\circ\text{C}$ ) appears to cause a reduction in barrier height and a decrease in barrier uniformity. After bake-out, typical barrier heights are about 1.25 eV maximum. Thus, even if there were no electron scattering in an interfacial contaminating layer, the vast majority of the hot electrons injected into the metal have energies of only about 0.8 to about 1.25 eV.

Finally, there is the question of the transmission of electrons through the BaO activation into the vacuum. The exact thickness of the BaO films for optimum photoelectric emission is not known, but is believed to be about 25 monolayers. From metal/semiconductor contact theory, one can expect an energy diagram as shown in Fig. 28. The BaO forms a very high Schottky barrier in combination with the metal, owing to the very low electron affinity of BaO. The Schottky barrier is quite thin, however, because of the high donor density (deep donors) generally present in BaO. Thus, for hot electrons from the metal to enter the vacuum, the electrons must first penetrate the Schottky barrier into the conduction band of the BaO. Then they must traverse the BaO layer to



TA-5511-91

FIG. 28 PROPOSED ENERGY DIAGRAM FOR A THIN FILM OF BaO ON METAL

the vacuum without scattering, energy loss, or momentum changes. The overall probability of a hot electron in the metal entering the vacuum can be expressed in terms of a transmission coefficient  $T$ . It can be expected that  $T$  would be a strong function of the energy of the hot electrons. For energies below the vacuum level,  $T$  would be zero or very nearly zero for some reasonable external vacuum field. At and immediately above the vacuum level,  $T$  would be small for two reasons. First, the tunneling probability through the Schottky barrier would be relatively low. Second, any scattering, such as by acoustical or optical phonons, would reduce the energy of the electrons below the vacuum level and/or redirect the momentum of the electrons away from the acceptable emission angles.

As the energy of the hot electrons in the metal is increased,  $T$  would be expected to increase for two reasons. First, the transmission probability through the Schottky barrier would increase. Second, some energy loss could be sustained and the electrons still left with enough



energy to enter the vacuum. At sufficiently high energies, the electrons could essentially diffuse through the BaO and into the vacuum.

On examining the photoemission data for BaO on metals, it is possible to interpret the data as follows. For high values of  $h\nu$ , the photoelectrons originate from the metal because for the higher-energy electrons,  $T$  is high. As the photothreshold is approached, however, the number of photoelectrons originating from the metal decreases drastically owing to the rapid decrease in  $T$ , and the actual photoemission observed begins to be dominated by electrons originating from the BaO itself.

An alternative to BaO that should avoid the foregoing complications is a monolayer of cesium on the metal. This would result in a relatively unstable structure, however, and is not recommended. A more desirable approach would be to find a semiconductor that produces a much higher Schottky barrier than those produced by GaP ( $\sim 1.4$  eV). If Schottky barriers of 2.0 to 2.5 eV could be produced, a workable cathode using BaO activation might be feasible. It should be pointed out, however, that the mean free path of the hot electrons in the metal film would be lower at the higher energies, thus causing some reduction in efficiency.

#### B. Transistor Cathode

Only a preliminary amount of effort has been expended in the area of the transistor cathode, so that few conclusions can be stated at this time. It does appear, however, that the difficulties discussed above for BaO on metals applies, and perhaps even more strongly, to semiconductors. Owing to the low absorption coefficient for light in GaAs (until high values of  $h\nu$  are reached) most of the electrons excited into the conduction band of the GaAs are generated at a considerable depth from the surface. By the time they diffuse to the surface, their energy is essentially that corresponding to the bottom of the conduction band. At these low energies, the transmission coefficient  $T$  of the electrons through the BaO and into the vacuum is probably quite low, thus yielding a low quantum efficiency. One might expect, then, that the photoelectrons observed would originate predominantly from the BaO itself. The experimental data do, indeed, appear to confirm this conclusion.

### C. Transverse Field Emitter

The TFE constitutes a straightforward and direct approach to hot-electron emission. A simple explanation for the observed behavior is that at high fields, electrons tunnel from the negative electrode into the conduction band of the BaO, wherein some of them are accelerated to high energy levels. At sufficiently high fields, avalanche breakdown occurs, producing copious quantities of hot electrons and hot holes. Owing to the favorable device geometry employed, the escape probability for a hot electron into vacuum is quite high, thus leading to the high values of  $\alpha$  observed. Much more work on the TFE is required, however, to determine the exact physical mechanisms involved and the overall usefulness of the cathode in various practical applications.

### D. General Conclusions

The dipole theory of BaO barrier lowering appears to be invalid. The theory presented above in terms of a semiconductor energy diagram is much more in accord with the experimental data obtained during the course of this program. A particularly pertinent example is the fact that the work function after BaO deposition is almost completely independent of the work function of the substrate before activation. Another example is the requirement for a BaO layer of several monolayers thickness in order to achieve a low work function.

The surface-barrier and transistor cold cathodes would be more feasible if a work function lower than what has been obtained so far from a straight BaO evaporation could be achieved. A particularly attractive possibility is to dope the BaO heavily with shallow donors. This would make the BaO Schottky barrier thinner, thus improving the tunneling probability of hot electrons from a metal or semiconductor substrate into the BaO conduction band. In addition, the thinner Schottky barrier would enable a thinner BaO film to be used for a low-work-function condition, thus increasing the probability of transmission from the BaO conduction band into the vacuum. Finally, the work function itself could be reduced by several tenths of an eV. Calculations by Gorman<sup>10</sup> indicate that a work function on the order of 0.8 eV should be achievable

by doping heavily with a rare earth metal. Gorman tried without success to demonstrate such a reduction in work function. Gorman's experimental approach was highly questionable, however. It is believed that a straightforward co-evaporation should accomplish the desired doping. If successful, such an accomplishment would not only make the cold cathode schemes more attractive, but an infrared photocathode and a low-temperature thermionic emitter might be possible outgrowths of such work.

#### IV RECOMMENDATIONS FOR FURTHER WORK

##### A. Schottky Barrier Cathode

- (1) Continue development of techniques for fabricating metal/semiconductor diodes that fit Schottky theory.
- (2) Continue study of BaO activation of metals.

##### B. Transistor Cathode

- (1) Study semiconductor materials that look promising for application to the p-n junction cathode.
- (2) Continue study of BaO activation of semiconductors.
- (3) Develop techniques for fabrication of complete cathode structures.

##### C. Transverse-Field Emitter

- (1) Conduct experimental and theoretical studies of wide-band-gap, low-electron-affinity semiconductors suitable for the TFE.
- (2) Continue with the development of techniques for fabrication of TFEs.

## REFERENCES

1. D. V. Geppert and B. V. Dore, "Research on Cold Cathodes," Second Quarterly Report, SRI Project 5511, Contract NAS 5-9581, Stanford Research Institute, Menlo Park, California (November 1965).
2. D. V. Geppert and B. V. Dore, "Research on Cold Cathodes," First Quarterly Report, SRI Project 5511, Contract NAS 5-9581, Stanford Research Institute, Menlo Park, California (August 1965).
3. D. V. Geppert, A. M. Cowley, and B. V. Dore, "Correlation of Metal/Semiconductor Barrier Height and Metal Work Function; Effects of Surface States," to be published in J. Appl. Phys.
4. D. V. Geppert and B. V. Dore, "Cold Cathodes for Low-Noise TWT Applications," Final Report, SRI Project 5175, Contract SRI 010165, Stanford Research Institute, Menlo Park, California (September 1965).
5. D. V. Geppert and B. V. Dore, "Research on Cold Cathodes," Third Quarterly Report, SRI Project 5511, Contract NAS 5-9581, Stanford Research Institute, Menlo Park, California (February 1966).
6. G. E. Moore and H. W. Allison, Phys. Rev. **77**, p. 246 (1950).
7. J. J. Scheer and J. van Laar, Solid State Comm. **3**, p. 189 (1965).
8. J. Burton, Phys. Rev. **108**, p. 1342 (1957).
9. Eim, Pell, Phys. Rev. **87**, p. 457 (1952).
10. J. K. Gorman, J. Appl. Phys. **33**, p. 3170 (November 1962).